Regulation of Interpolar Microtubules by Microtubule Plus-End Binding Proteins in *Saccharomyces cerevisiae*

Eliott Robison Davidson

A dissertation

submitted in partial fulfillment of the

requirements for the degree of

Doctor of Philosophy

University of Washington

2013

Reading Committee:

Trisha Davis, Chair

Linda Breeden

Bonny Brewer

Program Authorized to Offer Degree:

Molecular and Cellular Biology

University of Washington

Abstract

Regulation of Interpolar Microtubules by Microtubule Plus-End Binding Proteins in *Saccharomyces cerevisiae*

Eliott Robison Davidson

Chair of the Supervisory Committee:

Trisha N. Davis, PhD.

Department of Biochemistry

Cells carrying out mitosis must ensure that each daughter cell receives a full complement of chromosomes. As part of this process, multiprotein complexes called kinetochores link centromeric DNA to microtubule plus ends. This attachment allows cells to carry out two tasks that are essential for proper chromosome segregation. It couples chromosome position to microtubule plus end dynamics to allow maneuvering of chromosomes. It also senses whether chromosomes have been correctly attached to the spindle, correcting errors and delaying the cell cycle as necessary. That the kinetochore can maintain attachment to a microtubule plus end that is constantly polymerizing and disintegrating under its grip is one of the kinetochore's more extraordinary feats. Why evolution has chosen to utilize the plus-end, one of the cell's most ephemeral structures, as the site of its crucial chromosomal attachments is unknown.

My lab previously isolated a *Saccharomyces cerevisiae* kinetochore mutant, *DAM1-765*, whose kinetochores retain their initial lateral attachment to the microtubule lattice instead of maturing into end-on attachments. Despite this fundamental defect in spindle

organization, *DAM1-765* cells proliferate nearly as rapidly as wild-type. To determine how end-on kinetochore-microtubule attachments benefit the cell, I performed a synthetic lethal screen against *DAM1-765*. This screen produced mutant alleles of the EB1 homolog Bim1, CLIP-170 homolog Bik1, and the kinesin-14 subunits Kar3 and Cik1. Cells possessing these mutations fail to properly bundle spindle microtubules and struggle to biorient chromosomes, phenotypes which are exacerbated in the presence of *DAM1-765.* The presence of a kinetochore capping the plus end of a kinetochore microtubule appears to assist in the proper development of interpolar microtubules. In the absence of such a cap, spindle microtubules are poorly organized, and spindles are short and subject to collapse.

Three proteins identified in my synthetic lethal screen, Bim1 and Kar3/Cik1, are believed to be involved in bundling and regulating interpolar microtubules. It is unknown, however, how these proteins accomplish these tasks when they are only known to be able to bind to a single microtubule. I have identified a potential Bim1 binding motif, SxIP, on Cik1's N-terminus. This motif is highly conserved among kinesin-14s. To determine the role this motif plays in kinesin-14 function on the mitotic spindle, I mutated this motif to alanine residues and assayed the mutation's effect on spindle structure via fluorescence microscopy. The motif is important for recruitment of Cik1 to the spindle and for maintenance of proper spindle length in both metaphase and anaphase. The existence of a greater Bim1/Kar3/Cik1 complex capable of binding to two microtubules (one via Bim1's calponin homology domain, and one via Kar3/Cik1's motor and motor homology domains) could explain how Bim1 and Kar3/Cik1 are able to bundle interpolar microtubules together.

This work confirms that Bim1, Kar3, and Cik1 are important bundlers and regulators of interpolar microtubules and raises the possibility that Bik1 may be involved in this process as well. It suggests a mechanism by which Bim1 and Kar3/Cik1 may carry out these tasks. It also demonstrates that regulation of the different cohorts of spindle microtubules is

intimately linked; interpolar microtubules rely on the proper maturation of kinetochore microtubules to properly develop themselves.

Table of Contents

Page

List of Figures

Page

List of Tables

Page

Acknowledgments

I would like to thank Kristen Greenland, Michelle Shimogawa, Megan Wargacki, and Gefeng Zhu for strains, Susan Francis, Jerry Tien, and Per Widlund for plasmids, Kim Fong for assistance with Illumina sequencing, and Michelle Shimogawa for previously published work on this project. Anne Knowlton deserves special mention for wondering whether Cik1 contains a SxIP motif. Trisha Davis, Mike Ess, Eric Muller, and Mike Riffle wrote software I used extensively for data analysis. All members of the Davis Lab, especially Kim Fong, Beth Graczyk, Kristen Greenland, Anne Knowlton, Emily Mazanka, Eric Muller, Richard Ramsden, Michelle Shimogawa, Jerry Tien, and Megan Wargacki provided valuable scientific discussion. I'm grateful to Linda Breeden, Bonny Brewer, Trisha Davis, and Billie Swalla for serving on my advisory committee. And above all I'd like to thank Trisha Davis for the generous and unwavering guidance, support, and funding that saw me through this project.

Chapter I

Introduction

Whenever a cell divides, it must ensure that each of the new daughter cells receives a correct set of chromosomes. To accomplish this segregation, a massive molecular machine called the mitotic spindle assembles itself from thousands of individual protein subunits and attaches to each chromosome while signaling the cell to delay mitotic progression. Once all chromosomes are correctly attached, it pulls the chromosomes into each daughter cell. Most of the spindle then disassembles. The intricate maneuvers of the chromosomes and mitotic spindle during mitosis fascinated the earliest cell biologists, though they did not know why cells took such care to divide their chromosomes exactly in half (Wilson, 1925). They also noted that the process often seemed to go awry in tumors, a hallmark trait of cancer cells whose significance is still debated today (Venkitaraman, 2007; Wilson, 1925).

Spindle Assembly: Kinetochore Biorientation

To properly segregate chromosomes in anaphase, the mitotic spindle must link sister chromatids to opposite spindle poles, a process known as biorientation. Chromosomes are attached to the spindle via multiprotein structures called kinetochores which assemble on centromeric DNA. Kinetochores are themselves remarkable machines that carry out multiple functions during mitosis: they must bind to both DNA and microtubules to link chromosomes to the spindle, stay attached to the tip of their microtubule(s) as it polymerizes and depolymerizes underneath their grip, and release the microtubule if they form an improper attachment. The mechanisms underlying these feats have been the topic of intense study.

The initial interaction between a kinetochore and a microtubule typically occurs not at the microtubule tip, but on the side of the microtubule lattice (Rieder and Alexander, 1990). Kinetochore-microtubule binding is thought to be mediated via the Ndc80 and Dam1 complexes of the kinetochore (Asbury et al., 2006; Powers et al., 2009; Tanaka and Desai, 2008; Tien et al., 2010). After initial capture, the kinetochore is transported poleward, presumably by microtubule motors (Rieder and Alexander, 1990; Tanaka et al., 2005), and transitions from the initial lateral microtubule attachment to an end-on attachment at some point before anaphase (Lampson et al., 2004; Tanaka et al., 2007) (See Figure 1.1). Properly bioriented pairs of sister kinetochores will be under tension as their respective microtubules tug them toward opposite poles. This tension appears to be an important signal to the cell to stabilize the microtubule-kinetochore attachment (Nicklas and Ward, 1994); kinetochores that are not under tension (possibly because they are attached to the same pole) are attached more weakly and eventually release, free to form a new, correct attachment (Pinsky et al., 2006). Kinetochores that are not bioriented also emanate a signal to the cell to delay anaphase. Once all kinetochores are bioriented, that signal is silenced, and the cell is free to complete mitosis.

Spindle Assembly: Interpolar Microtubules

In order for all the above spindle functions to occur, however, the two spindle poles must be separated and kept separated even against the tugging forces exerted by the stretched DNA of bioriented sister chromatids. This function is carried out by interpolar microtubules, microtubules that emanate from each pole and are bundled together in the central spindle to form rigid struts that maintain and regulate pole separation.

During S phase, the spindle pole duplicates, forming two side-by-side poles. Microtubules emanate from these poles, interdigitate, and, assisted by kinesin motors, form an

antiparallel array to separate spindle poles (Hagan and Yanagida, 1990). Several classes of proteins bundle these antiparallel microtubules together, preventing spindle collapse and regulating spindle length. During anaphase, interpolar microtubules polymerize rapidly and slide against one another to push the poles further apart and maneuver chromosomes into the two daughter cells (McIntosh et al., 1985).

The identities of many interpolar-microtubule bundling proteins have been identified in budding yeast, though their exact functions remain unknown. These include the plus-end-directed homotetrameric kinesins Cin8 and Kip1, the nonmotor protein Ase1, the microtubule end-binding protein Bim1, and the minus-end-directed heterodimeric kinesin Kar3/Cik1 (Barrett et al., 2000; Gardner et al., 2008; Kotwaliwale et al., 2007; Saunders and Hoyt, 1992).

Microtubule Bundling and Plus-End Binding Proteins

Microtubules comprise one of the core cytoskeletal components of the cell. They are highly dynamic structures, switching stochastically between phases of polymerization and depolymerization, which in yeast occur primarily at the microtubule plus end (Maddox et al., 2000). The length of microtubules *in vivo* is highly regulated, however. There is a large number of proteins that bind to microtubules to regulate microtubule length and position. In the context of yeast mitosis, these fall into three general categories: kinesin motors, plus-end binding proteins, and the non-motor proteins Ase1 and Stu1.

To function as a machine for capturing, biorienting, and separating sister chromatids, the spindle must maintain a length appropriate for the task it is carrying out. In yeast, spindle length is determined by three main forces: an outward (lengthening) force generated by plus-end-directed kinesin motors acting on antiparallel interpolar microtubules, an inward (shortening) force generated by minus-end-directed kinesins on those same microtubules,

and another inward force generated by the stretched chromatin of bioriented chromosomes (Goshima and Scholey, 2010). All three of these forces are tied intimately to regulation of microtubule length: kinetochore microtubule length in the case of chromatin stretch, and interpolar microtubule length and overlap in the case of kinesin motors. My work has focused mainly on regulation of interpolar microtubules.

Three classes of microtubule plus-end binding proteins act as core regulators of microtubule dynamics, each of which has a single member in yeast: Bim1 (human homolog EB1), Bik1 (CLIP-170), and Stu2 (XMAP215). These proteins are capable of binding to microtubule plus ends, to each other, and often to accessory proteins that they recruit to the plus end (Akhmanova and Steinmetz, 2008; Wolyniak et al., 2006). The presence of these proteins can promote either microtubule polymerization or depolymerization depending on the context (Akhmanova and Steinmetz, 2008), and their direct effect is often unclear. Bik1 and Bim1 are often found together at microtubule plus ends, for instance, but it is unknown whether Bik1/Bim1 binding allows Bik1 to act on the plus end or sequesters Bik1 from it (Blake-Hodek et al., 2010).

The outward and inward forces acting on interpolar microtubules are generated in budding yeast by three different kinesin motors. The minus-end-directed motor Kar3/Cik1 is a kinesin-14 that localizes to microtubule plus ends and provides the inward, shortening force (Saunders et al., 1997; Sproul et al., 2005). This force is antagonized by the plus-end-directed kinesin-5 motors Cin8 and Kip1, which act on the microtubule lattice (Saunders et al., 1997). Cin8 and Kip1 appear to be largely redundant, though Kip1 becomes more dominant in the second part of anaphase B (Straight et al., 1998).

Two other proteins, Ase1 and Stu1, are neither kinesins nor plus-end binding proteins, yet still play important roles at interpolar microtubules. Ase1 is a highly conserved protein that

binds to the microtubule lattice and acts to bundle multiple microtubules to each other and also serves as a brake against kinesin-induced microtubule sliding (Braun et al., 2011). Stu1 binds to the microtubule lattice once kinetochores become attached to the spindle and is necessary to allow Cin8 to generate its outward force (Ortiz et al., 2009; Yin et al., 2002).

Spindle Checkpoint

In order for each daughter cell to receive one copy of each chromosome, the cell must ensure that all pairs of sister chromatids have been bioriented on the spindle. This verification process is carried out at the kinetochore by the proteins of the spindle checkpoint, which act to destabilize incorrect kinetochore-microtubule attachments and also signal the cell to delay anaphase until all chromosomes have been correctly attached to the spindle. A critical trait sensed by the yeast kinetochore appears to be tension (Pinsky and Biggins, 2005). Yeast kinetochores are only ever under tension when they are correctly bioriented, so the absence of tension at a given kinetochore means that its chromosome has not yet been correctly attached to the spindle. Kinetochores that are not under tension are phosphorylated on the Ndc80 and Dam1 complexes by the Ipl1 kinase, rendering the kinetochore incapable of forming long-lasting attachments to spindle microtubules (Cheeseman et al., 2002; Gestaut et al., 2008; Pinsky et al., 2006; Tien et al., 2010). This low microtubule affinity allows them to detach and re-attach in a manner that may correctly biorient them. Non-bioriented kinetochores also act as centers to convert the Mad2 protein into its active form, which signals the cell to halt cell cycle progression (Chan et al., 2005). Once kinetochores biorient and come under tension, Ipl1 ceases to phosphorylate the Ndc80 and Dam1 complexes, possibly due to a tension-induced conformational change of the kinetochore (Cimini et al., 2006; Lampson and Cheeseman, 2011). The subsequent dephosphorylation of the Ndc80 and Dam1 complexes results in stronger and more enduring kinetochore-microtubule attachment. The spindle checkpoint proteins responsible for Mad2

activation are also transported away from the kinetochore (Chan et al., 2005), resulting in Mad2 inactivation, permitting the cell to enter anaphase.

The Dam1 Complex

The Dam1 complex is one of two protein complexes that form the main load-bearing attachments between the yeast kinetochore and its microtubule (Asbury et al., 2006; Powers et al., 2009; Tanaka and Desai, 2008; Tien et al., 2010). It is composed of ten different essential protein subunits (Salmon, 2005), including its namesake, the protein Dam1. It is thought to coat spindle microtubules, possibly forming a ring structure (Gestaut et al., 2008; Miranda et al., 2005; Westermann et al., 2005) and then associate with the kinetochore after initial microtubule capture (Li et al., 2002). It is highly phospho-regulated by both the Ipl1 and Mps1 kinases. As mentioned above, phosphorylation by Ipl1 plays a role in the spindle checkpoint and in correcting microtubule attachment errors. Phosphorylation by Mps1 appears to have a role in allowing the kinetochore-microtubule attachment to mature from a lateral attachment into a plus-end one (Shimogawa et al., 2006).

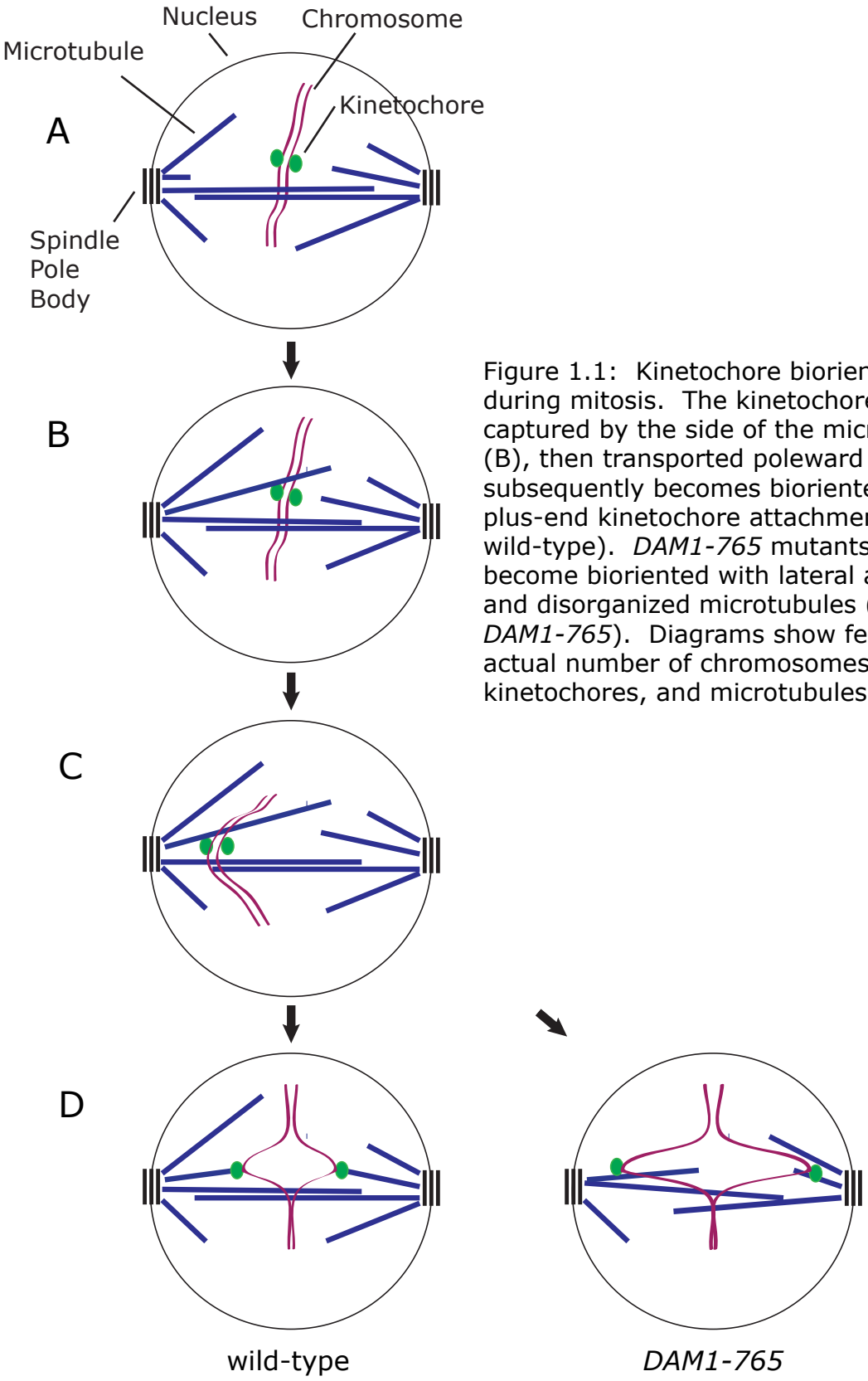

Figure 1.1: Kinetochore biorientation during mitosis. The kinetochore is initially captured by the side of the microtubule (B), then transported poleward (C), and subsequently becomes bioriented with plus-end kinetochore attachments (D, wild-type). *DAM1-765* mutants instead become bioriented with lateral attachments and disorganized microtubules (D, *DAM1-765*). Diagrams show fewer than actual number of chromosomes, kinetochores, and microtubules for clarity.

Table 1.1: Glossary of Frequently-Mentioned Spindle Components

Protein	Role
Ase1	Nonmotor bundler of interpolar microtubules
Bik1	Microtubule plus-end-binding protein. Regulates plus-end dynamics.
Bim1	Microtubule plus-end-binding protein. Regulates plus-end dynamics and assists in bundling interpolar microtubules.
Cik1	Minus-end-directed kinesin subunit. Pairs with Kar3 to bundle interpolar microtubules.
Cin8	Plus-end-directed kinesin motor. Bundles interpolar microtubules and exerts outward (spindle-lengthening) force on them. Largely redundant with Kip1.
Dam1	An essential microtubule-binding component of yeast kinetochores
Kar3	Minus-end-directed kinesin motor. Dimerizes with either Cik1 or Vik1. Bundles interpolar microtubules and exerts inward (spindle-shortening) force on them.
Kip1	Plus-end-directed kinesin motor. Bundles interpolar microtubules and exerts outward (spindle-lengthening) force on them. Largely redundant with Cin8.
Stu1	Nonmotor protein. Potentiates Cin8 unless sequestered by unattached kinetochores.
Tub1	Tubulin, the structural subunit of microtubules
Vik1	Minus-end-directed kinesin subunit. Pairs with Kar3.

Chapter II

Kinetochore Attachment to Kinetochore Microtubule Plus Ends is Necessary for Proper Regulation of Interpolar Microtubules on the Mitotic Spindle

Introduction

Several years ago, the Davis lab isolated an interesting allele of Dam1 in a screen for mutants that were sensitive to weakened spindle pole bodies (Shimogawa et al., 2006). This allele, *DAM1-765*, encodes the substitution S221F, which removes one of several Mps1 phosphorylation sites on the Dam1 protein, with severe consequences for the organization of the spindle (Shimogawa et al., 2006). *DAM1-765* metaphase spindles are shorter as measured from pole to pole than wild-type spindles (Shimogawa et al., 2006). Despite this shortening, they stretch sister kinetochores farther apart in metaphase than wild-type cells do, raising the possibility that the kinetochores, being stretched unusually far apart, are exerting unusually strong inward force on the spindle pole bodies (Shimogawa et al., 2006). Spindle microtubules in *DAM1-765* cells are also oddly disorganized (Shimogawa et al., 2006). In wild-type metaphase spindles, roughly twenty microtubules emanate from each spindle pole body: sixteen short microtubules, each with a kinetochore attached to the tip, and four pole-to-pole microtubules (Winey et al., 1995). Electron tomography of *DAM1-765* spindles, however, reveals that they only contain sixteen microtubules per pole total, and that those microtubules are of random length (Shimogawa et al., 2006). The combination of altered kinetochore clustering and random microtubule length render it impossible for most *DAM1-765* kinetochores to be attached to the tip of a microtubule; most must remain laterally attached (Shimogawa et al., 2006). Despite skipping the transition from lateral to end-on attachment, however, *DAM1-765* cells display little growth defect (Shimogawa et al., 2006; Shimogawa et al., 2010).

The *DAM1-765* allele could potentially be a useful tool for learning more about kinetochore capture and biorientation in mitosis. I have been particularly interested in exploring why cells go to considerable effort to perform what must be a complicated transition from lateral to end-on attachments. If lateral attachments perform well, as the *DAM1-765* allele appears to show, it would be surprising for the transition to be conserved throughout eukaryotic evolution. And the microtubule plus end, an ephemeral structure that is incessantly adding or losing subunits, is a counterintuitive site for the cell's crucial chromosomal attachments. My work has focused on discovering what deleterious consequences failure to make end-on attachments has for cells.

Results

Synthetic Lethal Screen against DAM1-765

To determine what vulnerabilities *DAM1-765* confers on cells, I performed a synthetic lethal screen against *DAM1-765* as described in Materials & Methods. The screen produced mutations in four genes: the microtubule plus-end-binding proteins Bik1 and Bim1 (homologs of human CLIP-170 and EB1, respectively), and both subunits of the kinesin-14 Kar3/Cik1. All mutants produced by the screen were found to have single point mutations in the above genes which are summarized in Table 2.1. I selected *bik1-19, bim1-16, cik1-12,* and *kar3-8* for further study. *bik1-19* contains a missense mutation in Bik1's CAP_GLY domain, which binds both microtubules and EB-family proteins (Berlin et al., 1990; Dujardin et al., 1998; Weisbrich et al., 2007). *bim1-16* mutates an arginine residue homologous to R17 in human EB1, a residue known to be critical for Bim1's association with microtubules (Slep and Vale, 2007). *cik1-12* mutates a residue in Cik1's N-terminal tail, just upstream from its coiled-coil dimerization domain (Allingham et al., 2007; Manning et al., 1999; Page and Snyder, 1992). *kar3-8* encodes a mutation in Kar3's C-terminal motor domain and is

the only temperature-sensitive allele isolated in the screen (Gulick et al., 1998; Meluh and Rose, 1990). *DAM1-765 kar3-8* cells are viable at 30ºC and dead at 37ºC.

Interdependence of Bik1, Bim1, and Kar3/Cik1 for spindle localization

One of Bim1's roles is to recruit other proteins to the mitotic spindle (Akhmanova and Steinmetz, 2008). It was therefore possible that the synthetic lethality of *bim1-16* was due to a defect in recruitment of Bik1 or Kar3/Cik1 to the spindle. To determine whether Bik1, Bim1, and Kar3/Cik1 depend on one another for spindle localization, I assessed the total metaphase spindle fluorescence of *BIK1-GFP*, *BIM1-CFP*, and *CIK1-GFP* in wild-type, *bik1-19*, *bim1-16*, and *cik1-12* backgrounds. *BIM1-CFP* displayed robust fluorescence in all mutant backgrounds analyzed (see Figure 2.1). Fluorescence in a *bik1-19* background was slightly (12%, $p<0.05$) higher than WT. *BIK1-GFP* fluorescence was consistent across backgrounds with the exception of *bim1-16*, which decreased *BIK1-GFP* fluorescence by 40% ($p<0.0005$). *CIK1-GFP* was highly sensitive to the presence of underlying mutations, with *bik1-19* and *bim1-16* decreasing fluorescence by 59% and 71%, (both $p<0.0005$), respectively. These results raise the possibility that the synthetic lethality of mutations in Bim1 and Bik1 with *DAM1-765* is due to their impact on Cik1 localization, but not vice versa.

I additionally attempted to create GFP-tagged *bim1-16* and *cik1-12* to determine whether those mutations affect the spindle localization of the proteins themselves. *bim1-16-GFP* failed to produce any perceptible spindle fluorescence, confirming that the arginine residue mutated in that allele is critical for Bim1 spindle localization. I was unsuccessful at creating *cik1-12-GFP*, presumably because adding a tag to the already-compromised *cik1-12* is lethal.

DAM1-765 kar3-8 cells undergo repeated spindle collapse

kar3-8's temperature sensitivity makes it an attractive tool to study *DAM1-765* synthetic lethality. Double mutant cells can be grown at the permissive temperature and then transitioned to the restrictive temperature to observe the lethal phenotype. As an initial inquiry into what consequences the *kar3-8* allele has for the spindle, I fluorescently labeled spindle poles and tubulin and observed *kar3-8* and *kar3-8 DAM1-765* spindles at 23C and 37C. At 23C, *DAM1 kar3-8* cells appear normal aside from some spindle positioning defects, as expected in a kinesin-14 mutant (Zaichick et al., 2009). Spindle length is indistinguishable from wild-type cells (see Figure 2.2). *DAM1-765 kar3-8* pre-anaphase spindles at 23C are markedly shorter than WT, however (see Figure 2.2). Time-lapse images of *GFP-TUB1* in the double mutant background show that the spindle poles appear locked in a cycle of pole separation followed by spindle collapse (see Movies 1A and 1B). At 37C, *kar3-8* pre-anaphase spindles appear short. *DAM1-765 kar3-8* spindle poles at 37º rarely separate at all (see Movie 2). *kar3-8* also prevents maintenance of a bipolar spindle; *kar3-8* cells synchronized at the permissive temperature in hydroxyurea, which arrests cells in S phase with short spindles, still suffer spindle collapse after transition to the restrictive temperature (see Figure 2.3). These observations, especially the V-shaped conformation adopted by collapsing *DAM1-765 kar3-8* spindles, suggest that *kar3-8* spindles may have a weakened array of interpolar microtubules.

Kar3 heterodimerizes with one of two accessory proteins: Cik1 or Vik1 (Manning et al., 1999). Only Cik1 appeared in the synthetic lethal screen, though screen coverage may have been insufficient to find all genes whose mutation is synthetic lethal with *DAM1-765.* I was concerned that *kar3-8* may be impacting function of Kar3/Vik1 and thus producing phenotypes unrelated to *DAM1-765* synthetic lethality. To avoid being distracted by pleiotropic effects, I developed a means of partially rescuing *bim1-16 DAM1-765* and *cik1-12 DAM1-765* and analyzed those strains.

Partially-rescued DAM1-765 double mutants exhibit short spindles and poor microtubule bundling

DAM1-765 is normally a dominant allele (Shimogawa et al., 2006). My synthetic lethal screen relied on a high copy number of plasmids containing *DAM1* to suppress *DAM1-765*'s dominant lethality. I found that supplying *DAM1* on a lower copy number, centromere-bearing plasmid would partially suppress synthetic lethality in *bim1-16 DAM1-765 [CEN DAM1]* and *cik1-12 DAM1-765 [CEN DAM1]* lines, resulting in slow growing strains that could be characterized. I included samples of *DAM1-765 kar3-8* grown at permissive temperatures in these analyses, since it is viable but also grows slowly and thus could also offer insight as to the mechanism of lethality in *DAM1-765* synthetic lethal mutants.

To determine whether the spindle collapse initially observed in *DAM1-765 kar3-8* cells was general to all *DAM1-765* synthetic lethal mutations, I measured spindle lengths of cells in asynchronous culture in WT, *DAM1-765*, the three relevant single mutants (*bim1-16, cik1-12,* and *kar3-8*), and in the three partially-rescued double mutant strains (see Figure 2.2). Wild-type spindles begin to expand rapidly at roughly 1.7 μm in spindle length (see Figure 2.2A), so spindles shorter than 1.7 μm were considered to be pre-anaphase for purposes of analysis. No strains display clear irregularities in anaphase (see Figure 2.2A). Before anaphase, however, all three double mutants have a striking defect in spindle length. Wild-type pre-anaphase cells have a mean length of 1.13 μm (see Figure 2.2B). The lengths of the spindles in the single mutants are not significantly different from WT ($p>0.05$, Tukey-Kramer method). In contrast, all three double mutants display short spindles, which cluster at 0.75-0.77 μm ($p<0.01$) in length.

Since pole separation is determined by a balance of outward forces acting on interpolar microtubules (ipMTs) and inward forces acting on kinetochores and ipMTs (Goshima and

Scholey, 2010; Sullivan and Huffaker, 1992), these data suggest that the double mutants may be suffering some sort of failure or misregulation of ipMTs, especially since Bim1, Cik1, and Kar3 are already known to play roles in ipMT bundling (Gardner et al., 2008). Cells with badly bundled (as opposed to merely shorter) ipMTs would be expected to have a less closely packed ipMT core and thus a wider distribution of spindle tubulin when the spindles are viewed longitudinally. To determine whether the partially-rescued *DAM1-765* double mutants had poorly-bundled ipMTs, I labeled cells with GFP-tubulin (GFP-TUB1) and measured spindle width as the diameter that encompassed 50% of observed GFP-TUB1 fluorescence in each strain (see Figure 2.4).

Early pre-anaphase WT spindles, defined for this analysis as spindles <1.1 μm in length, have a 50% intensity diameter of 231±2nm. *DAM1-765* is slightly broader at 261±4nm ($p<0.01$, Tukey-Kramer method), though that broadening is largely rescued by the introduction of *[CEN DAM1]* (241±2nm)($p<0.05$). All single mutants have a slight bundling defect, clustering between 251 and 265±3nm ($p<0.01$ each). *DAM1-765* double mutants score sharply higher, however, with *bim1-16 DAM1-765 [CEN DAM1], cik1-12 DAM1-765 [CEN DAM1],* and *DAM1-765 kar3-8* (23C) respectively displaying spindle widths of 303±6, 282±4, and 299±5nm ($p<0.01$ each, versus both WT and single mutants). Pre-anaphase spindles longer than 1.1 μm display the same pattern of diffuse bundling in double mutants, though the defect is generally not as pronounced (see Figure 2.4C). The broadening of tubulin distribution seen in each early pre-anaphase double mutant exceeds what would be expected if the mutations in the double mutants were each contributing small independent defects in an additive manner, suggesting that the double mutants' spindle broadening is a true synthetic phenotype.

Partially-rescued cik1-12 DAM1-765 is deficient in chromosome biorientation

Both *bim1-16 DAM1-765 [CEN DAM1]* and *DAM1-765 kar3-8* spindles frequently collapse in metaphase, producing V-shaped spindles that have folded in the mid-spindle. I have never observed this collapse in *cik1-12 DAM1-765 [CEN DAM1]* spindles, however. This difference raises the possibility that *cik1-12* may generate synthetic lethality through a mechanism other than ipMT collapse. Since *DAM1-765* kinetochores are uncoupled from the MT plus ends that normally generate the tension necessary to satisfy the spindle checkpoint, they may instead rely on minus-end-directed microtubule motors to generate that tension. Kar3 is the only minus-end-directed microtubule motor known to be present in the budding yeast nucleus and has been proposed to be the mechanism of poleward kinetochore transport (Tanaka et al., 2005). Kar3 is present in the nucleus in the form of two separate heterodimers (Kar3/Cik1 and Kar3/Vik1), but Vik1 appears to concentrate at spindle pole bodies rather than at kinetochores (Manning et al., 1999). A mutation in Cik1 could therefore result in difficulty with poleward transport in wild type cells and overall tension failure in a *DAM1-765* background.

Since tension is necessary to stabilize kinetochore-microtubule attachments (Pinsky et al., 2006), a strain unable to produce tension would be expected to suffer from frequent kinetochore detachment, resulting in difficulty separating sister kinetochores. To assess whether *cik1-12 DAM1-765 [CEN DAM1]* is deficient in kinetochore separation, I inserted an array of Lac operators at centromere 3 and viewed these cells in a background containing GFP fused to the Lac repressor. CEN3 is clearly illuminated in these strains, allowing measurement of centromere separation.

I found that in asynchronous culture, both *cik1-12* and *kar3-8* spindles are less frequently bioriented than WT spindles (see Figure 2.5A). Addition of a *DAM1-765* background further reduces the biorientation frequency of these alleles. Biorientation rates in *bim1-16* cells are

very low with and without *DAM1-765 [CEN DAM1]*. This pattern would be expected if Kar3 and Cik1, but not Bim1, were responsible for tension generation at *DAM1-765* kinetochores.

Biorientation frequency is highly dependent on spindle length, however. Very short spindles rarely have two discrete *CEN3* foci, while late metaphase spindles are nearly always bioriented (see Figure 2.5B). Since spindle length varies between the various alleles generated by the synthetic lethal screen (see Figure 2.2), I wanted to rule out variations in spindle length between strains as the cause of the observed changes in biorientation frequency. To account for spindle length variation, I binned the data presented in Figure 2.5A by spindle length and reanalyzed biorientation frequency (see Figures 2.5B and 2.5C). When viewed in this manner, a drop in biorientation frequency can still be observed in all single mutants analyzed. No further drop in biorientation occurs in the partially-rescued double mutants, however. The lack of a worsened phenotype in the double mutants when the data are binned by spindle length shows that the double mutants' reduced gross biorientation frequency is attributable to their reduced spindle length. The mutations identified in the synthetic lethal screen therefore do result in poor biorientation, but this phenotype is not exacerbated in a partially-rescued *DAM1-765* background. Kinetochore tension defects are thus unlikely to be the cause of *DAM1-765* synthetic lethality.

I was also curious whether the observed mutants fail to initiate biorientation or instead fail to maintain biorientation. To determine whether a failure to maintain biorientation contributes to the biorientation defect observed in our mutants, I filmed time-lapse videos of *cik1-12 DAM1-765 [CEN DAM1]* cells in asynchronous culture. *CEN3* foci were observed repeatedly separating a short distance and collapsing back together in small spindles, indicating a failure to maintain proper separation (see Movies 3A and 3B). These observations do not rule out the possibility that an initial biorientation delay may be contributing to the low number of bioriented spindles observed in this strain.

Discussion

DAM1-765 cells appear to have two prominent defects: misregulation of spindle microtubules that leads to poorly defined interpolar microtubules, and decoupling of kinetochores from microtubule plus ends (Shimogawa et al., 2006). Either of these features could plausibly contribute to cell death when paired with the mutations found in the synthetic lethal screen. *DAM1-765* interpolar microtubules could be less stable than normal and leave spindles vulnerable to further ipMT disruption, either through exacerbated misregulation of microtubule dynamics or impaired ability to bundle what few interpolar microtubules *DAM1-765* cells have. Alternatively, kinetochores that are laterally attached to microtubules have no obvious means of generating the tension necessary to satisfy the spindle checkpoint. They may be reliant on minus-end-directed microtubule motors to generate that tension (Tanaka et al., 2007), or may require proteins to stabilize their attachments that normally become irrelevant once the kinetochores convert to a tension-stabilized end-on configuration. Determining which of these mechanisms of synthetic lethality is at work in the screen-derived mutants (or discovery of a new mechanism) will shed light on why the dynamic microtubule plus end is the universal site of kinetochore attachment in mitotic cells.

Bim1, Cik1, and Kar3 are all thought to bundle ipMTs (Gardner et al., 2008). And Bik1, though not known to have a microtubule-bundling role, localizes to spindle microtubule plus ends (Shimogawa et al., 2006). On the other hand, kinesin-14s like Kar3/Cik1 are thought to mediate poleward kinetochore movement after initial capture in yeasts and to promote kinetochore biorientation (Gachet et al., 2008; Jin et al., 2012; Tanaka et al., 2005). Furthermore, Bik1's homolog CLIP-170 is involved in pre-metaphase kinetochore-microtubule attachment in human cells (Dujardin et al., 1998; Tanenbaum et al., 2006), though Bik1 itself is not present in large amounts at yeast *DAM1-765* kinetochores

(Shimogawa et al., 2006). Both kinetochore-based and ipMT-based mechanisms of synthetic lethality are plausible given the identities of some genes isolated in my screen, but only the ipMT-based mechanism can account for all four screen-identified genes.

The best clues regarding the mechanism(s) of synthetic lethality in the screen-derived mutations may come not just from examining the phenotypes of the single mutants, but from determining which of those phenotypes are enhanced in partially-rescued double mutants. These are the phenotypes that could reasonably worsen to a lethal extent in the true (dead) double mutants. The phenotypes that conform to this pattern point clearly to interpolar microtubule difficulties, not lack of tension at kinetochores, as the mechanism of *DAM1-765* synthetic lethality. The dramatic spindle collapses seen in *DAM1-765 kar3-8* cells and the diffuse pre-metaphase ipMT bundling seen in all three observed double mutants constitute direct evidence that ipMTs, already poorly bundled in *DAM1-765* spindles, are even more poorly bundled in a synthetic lethal background. Meanwhile, my biorientation assays failed to support the hypothesis that Kar3/Cik1 is necessary for tension generation in a *DAM1-765* background.

Exacerbation of interpolar microtubule bundling problems is therefore the most likely cause of synthetic lethality in the mutations obtained in my screen. This result is remarkable in that it suggests kinetochores bind to microtubule tips not because the tip is a particularly useful site for kinetochore attachment, but because having kinetochore-attached tips is an important step for the regulated self-assembly of the rest of the spindle. Perhaps having laterally attached kinetochores complicates the process of differentiation into populations of interpolar and kinetochore microtubules. Or perhaps the increased number of exposed microtubule tips robs true interpolar microtubules of critical tip-attached bundling factors or scarce tubulin subunits. In any case, kinetochore tip attachment appears to be necessary not for the direct health of the kinetochore or its attached chromatid, but for the health of

the spindle microtubules. The kinetochore can attach elsewhere on the spindle and still segregate safely, but the resulting microtubule disorganization risks the death of the cell.

Materials & Methods

Media

YPD medium was as previously described (Geiser et al., 1991). YPD 3x ade is YPD medium supplemented with additional adenine to a final concentration of 150 µg/ml. SD low ade is SD medium (Sherman et al., 1986) supplemented with 5 µg/ml adenine, 25 µg/ml uracil, 100 µg/ml tryptophan, and 0.1% casamino acids.

Synthetic Lethal Screen

The synthetic lethal screen was carried out using the red/white sectoring system described in (Muller, 1996). Strain EDY60 (*ade2 ade3 DAM1-765*) containing pED02 (*2 µm ADE3 DAM1*) was mutagenized to 0.5 lethal mutations per genome with ethylmethane sulfonate, plated on SD low ade media, and grown at 37ºC. Strains with mutations synthetic lethal to *DAM1-765* could not grow after loss of pED02 and therefore formed solid red colonies. To screen out dominant mutations, mutations in Shm2 (Nigavekar and Cannon, 2002), and Ade3 gene conversions, all mutants were mated to a *shm2* strain and checked for restored sectoring behavior. To screen out additional mutations at the Dam1 locus and mutations that were synthetically lethal with *lys2Δ,* plasmids pED5 and pSF15 (see Table 3.2) were transformed in parallel into all mutant lines. Only mutant lines that resumed sectoring under pSF15 and not under pED5 were retained.

Kar3 and Cik1 had been previously noted as high-likelihood genes and were identified via transformation of the mutant strains with plasmids bearing wild-type copies of those genes.

Bim1 was identified via transformation with a yeast genomic library constructed by Mark Rose.

Illumina high-throughput sequencing of mutant genomes identified Bik1. Two 5x-outcrossed isolates of the unidentified complementation group and an unmutagenized control were sequenced. Mutations in Bik1 were found via manual comparison of the wild-type and mutant sequence alignments in the Broad Institute's Integrative Genomics Viewer. Bik1 was confirmed as the relevant gene by transforming a *BIK1*-bearing plasmid into the *bik1 DAM1-765 pED2* double mutant strains and observing restored sectoring in those strains.

Mutant alleles were screened for temperature sensitivity by observing their sectoring behavior when grown at 23ºC. *bim1-16*, *cik1*-12, and *kar3-8* were reconstructed in an unmutagenized background as described below for further study.

Cloning

bim1-16, cik1-12, and kar3-8 were reconstructed in unmutagenized backgrounds using the pop-in/pop-out replacement technique (Rothstein, 1991) and verified via sequencing.

Fluorescent protein fusions and yeast transformations were performed as described on the Yeast Resource Center website (http://depts.washington.edu/yeastrc/). Fusion proteins were verified via sequencing.

Microscopy

Strains to be imaged were incubated overnight at ambient temperature (roughly 23ºC) on YPD 3x ade plates. They were then mounted on pads composed of SD complete media with 2% SeaKem Gold agarose and imaged with a DeltaVision microscope system (Applied Precision, Issaquah WA) containing an Olympus IL70 microscope, 100X, 1.35 numerical

aperture oil objective, CoolSNAP HQ digital camera (Photometrics, Tuscon AZ) and optical filter sets (Omega Optical, Semrock, and Chroma Technology).

Hydroxyurea Arrest

Kar3-8 cells were cultured in log phase for 24 hours and then arrested in 100 mM hydroxyurea for 1.5 doubling times at 23ºC. Cells were then imaged at 23ºC, heated to 37ºC for one hour, and imaged again.

Fluorescence Intensity

Fluorescence intensities were measured only from bipolar spindles with both poles in focus and quantified using software developed in-lab.

Time-Lapse Movies

Time-lapse images were taken with an interval of 6 seconds between frames.

Spindle Lengths

Distance between *SPC110-Cherry* foci was measured using the measurement tool in Applied Precision's softWoRx software suite.

CEN3 Biorientation

Cells with GFP-labeled CEN3 were prepared for microscopy as described above. Cells were imaged in Z stacks to ensure that all CEN3 foci were captured (18 panels per stack, 0.6 μm gap between panels). Z stacks were projected via the projection tool available in Applied Precision's softWoRx software suite. CEN3 foci were counted by hand.

Allele	Nucleotide Change	AA Change
bim1-16	G26A	R9H
bim1-105	C541T	Q181X
bim1-139	C208T	Q70X
bim1-146	G318A	W106X
bik1-19	G77A	G26D
bik1-40	G77A	G26D
bik1-50	G191A	S64N
bik1-121	C322T	Q108X
cik1-12	G226A	G76R
kar3-8 (ts)	G2149A	A717T
kar3-57	G298A	E100K
kar3-122	G298A	E100K

Table 2.1: Mutations identified in *DAM1-765* synthetic lethal screen

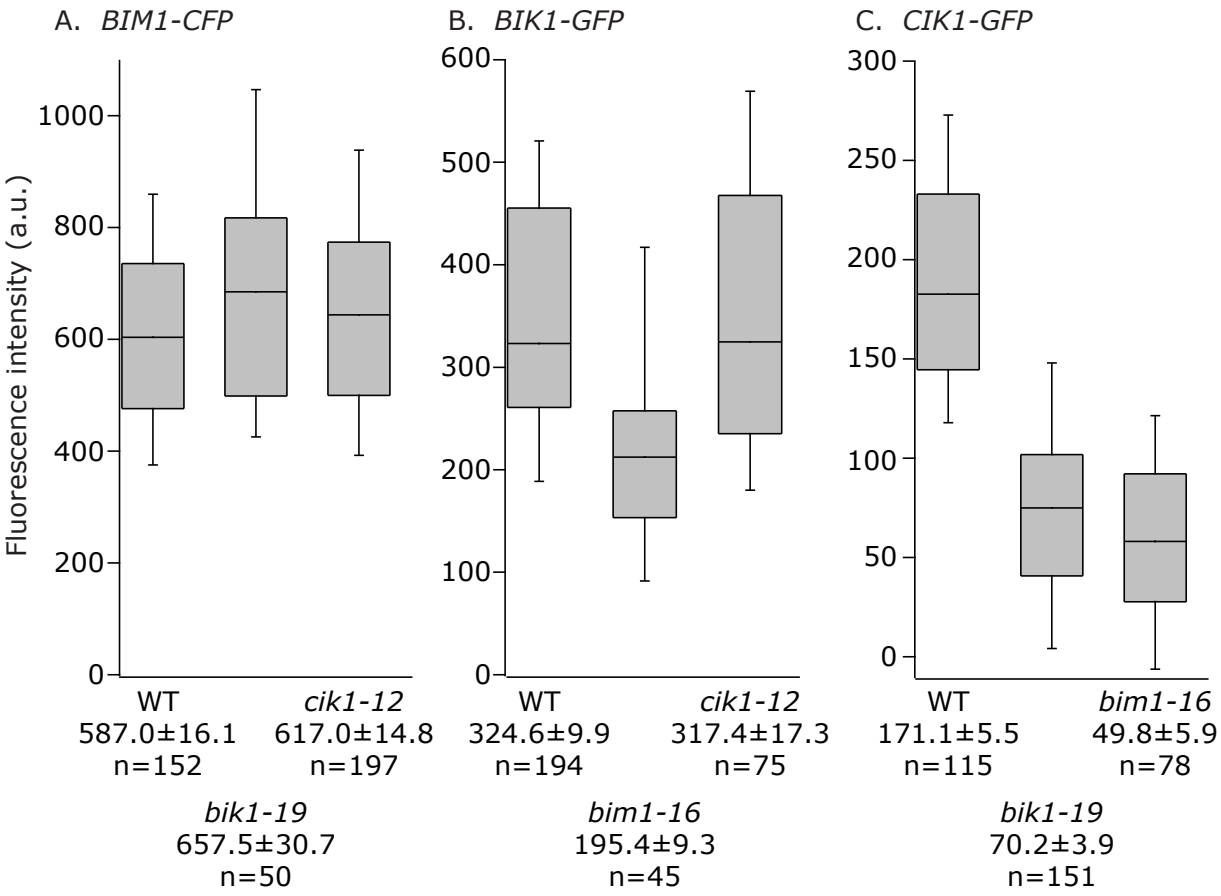

Figure 2.1: Metaphase spindle fluorescence of *BIK1-GFP*, *BIM1-CFP*, and *CIK1-GFP* in various backgrounds. Cells with fluorescently labeled spindle poles and the indicated fluorophore were incubated overnight at room temperature and then imaged in a single plane. Overall fluorophore spindle fluorescence intensity was measured in all spindles whose poles were in focus. Box plots indicate the median (inner line), 25th and 75th percentiles (box boundaries), and 10th and 90th percentiles (whiskers). X-axes display the genetic background, mean ± standard error as judged by Gaussian fit (arbitrary units), and n value. A: Intensity of *BIM1-CFP*. Fluorescence is relatively tolerant of background mutation. B: Intensity of *BIK1-GFP*. Fluorescence is reduced in a *bim1-16* background but not in *cik1-12*. C: Intensity of *CIK1-GFP*. Fluorescence is impacted by mutations in Bim1 and Bik1.

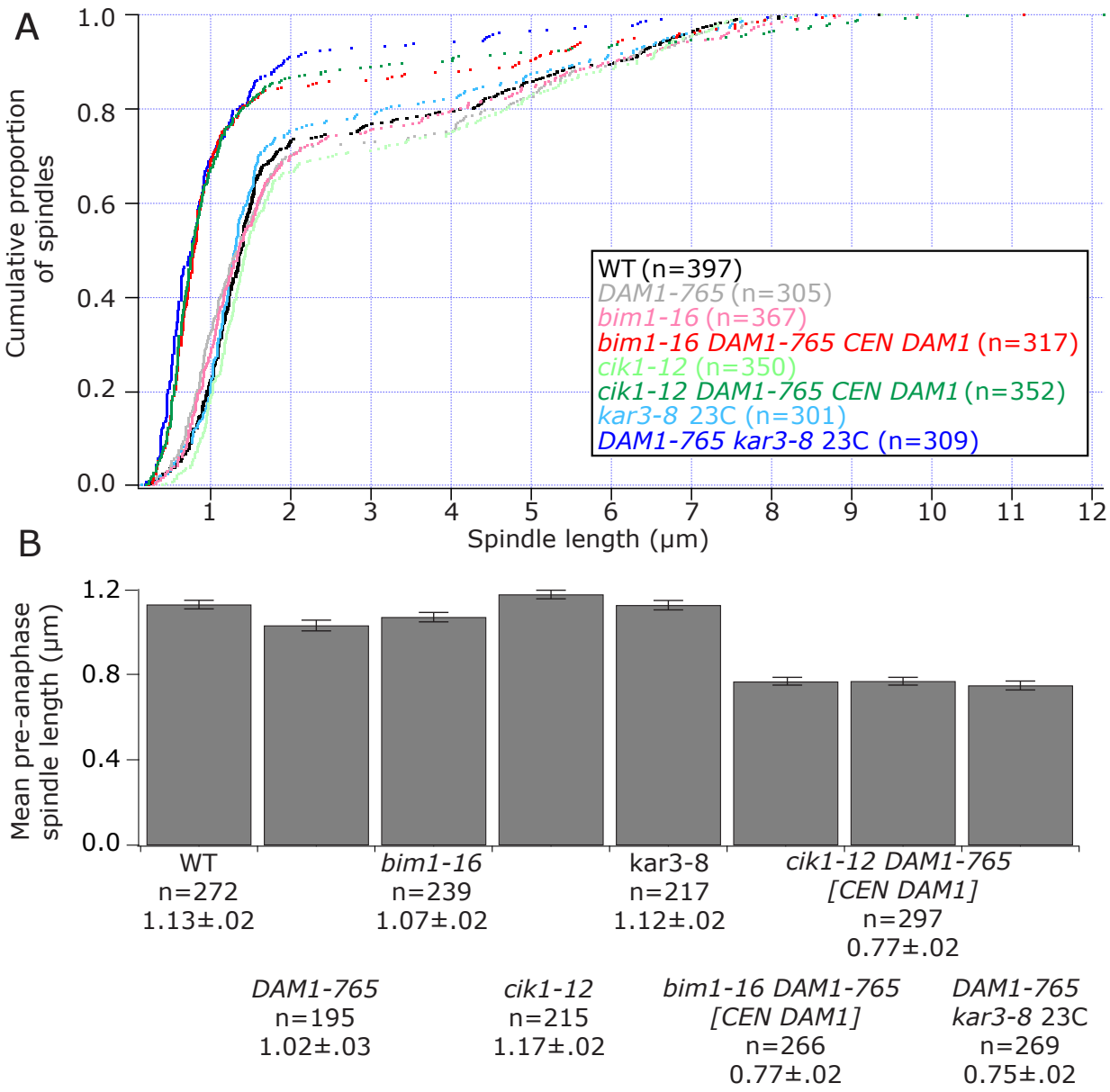

Figure 2.2: Spindle lengths of Bim1, Cik1, and Kar3 mutants in asynchronous culture. Cells with fluorescently labeled spindle poles and tubulin were incubated at room temperature overnight and then imaged in a single plane. Spindle length was measured in all cells with two poles connected by a track of tubulin. A: Data points ordered from smallest to largest and plotted on a cumulative distribution graph. Regions of increased slope are regions at which spindles more frequently appear and by inference are lengths at which spindle elongation slows. WT spindles pause pre-anaphase between 0.7 and 1.7 μm in length. All single mutants pause at lengths similar to WT. Double mutant spindles pause at shorter lengths (lower bound ~0.3 μm), and have a poorly resolved transition from metaphase to anaphase. Double mutant spindles also have a higher percentage of pre-anaphase spindles, indicating either a pre-anaphase delay or an increased rate of anaphase extension. B: Average lengths of pre-anaphase spindles from the same data set as part A. Error bars indicate standard error. Single mutants appear similar to WT, though double mutants are sharply shorter.

A

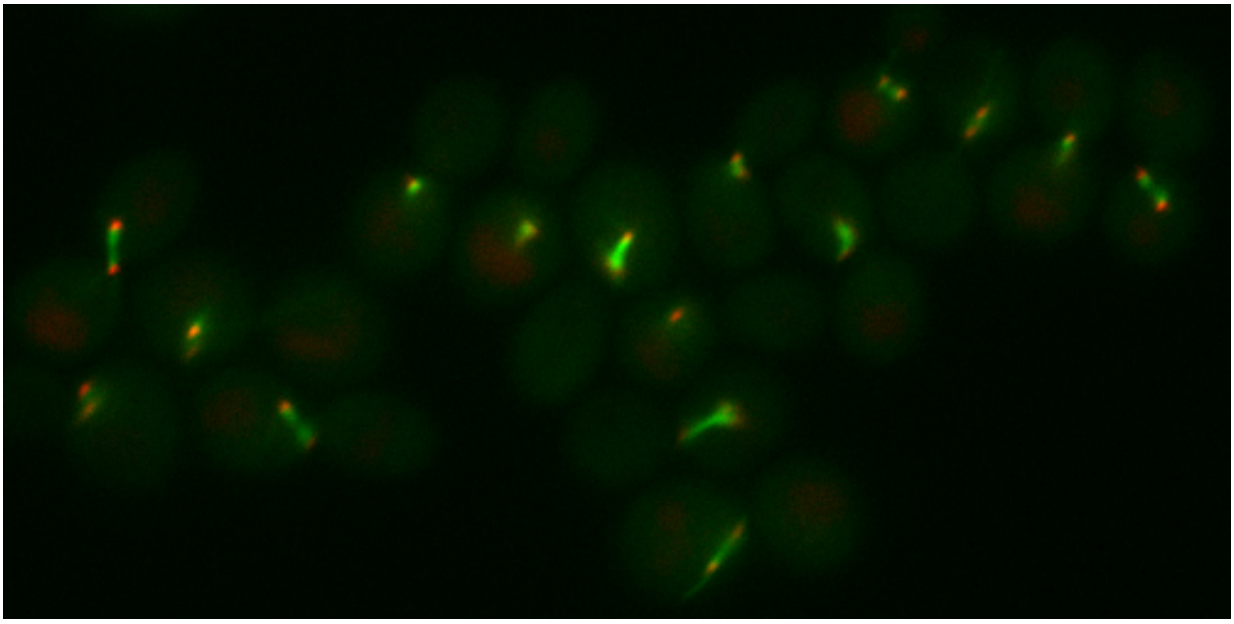

B

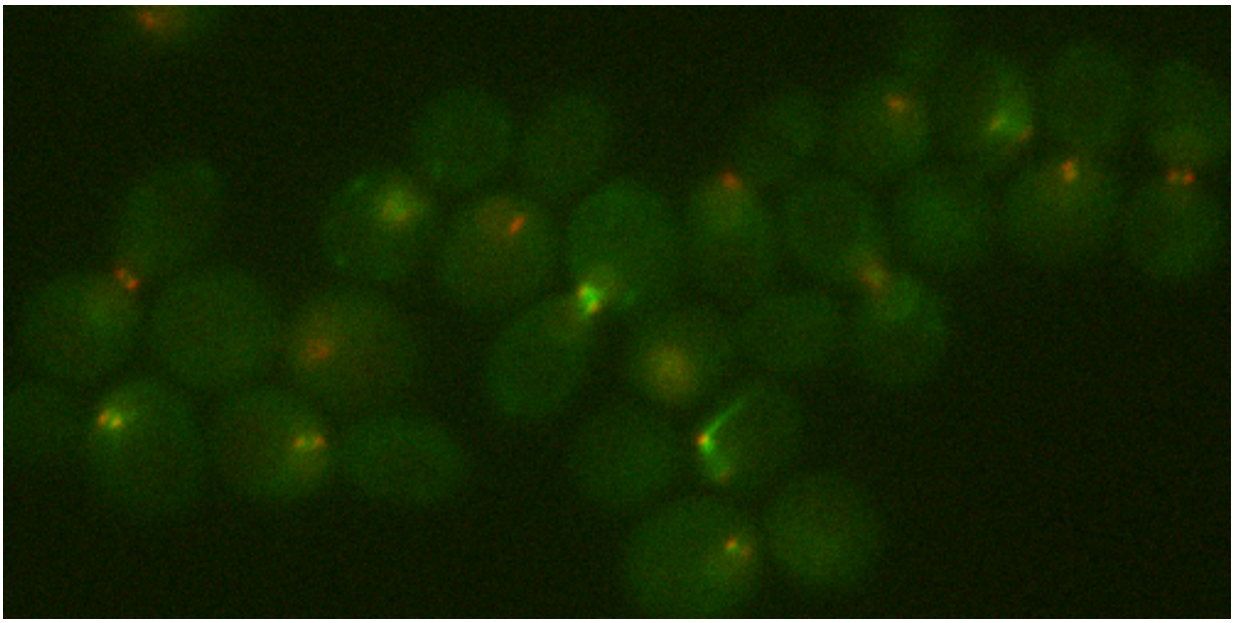

Figure 2.3: Hydroxyurea arrest of *kar3-8* cells. Spindle poles are fluorescently labeled with mCherry and tubulin is labeled with GFP. A: Arrested cells at 23C. Several spindles with well-separated poles can be seen. B: Arrested cells after 10 minutes at 37C. Most formerly large spindles are noticeably shorter.

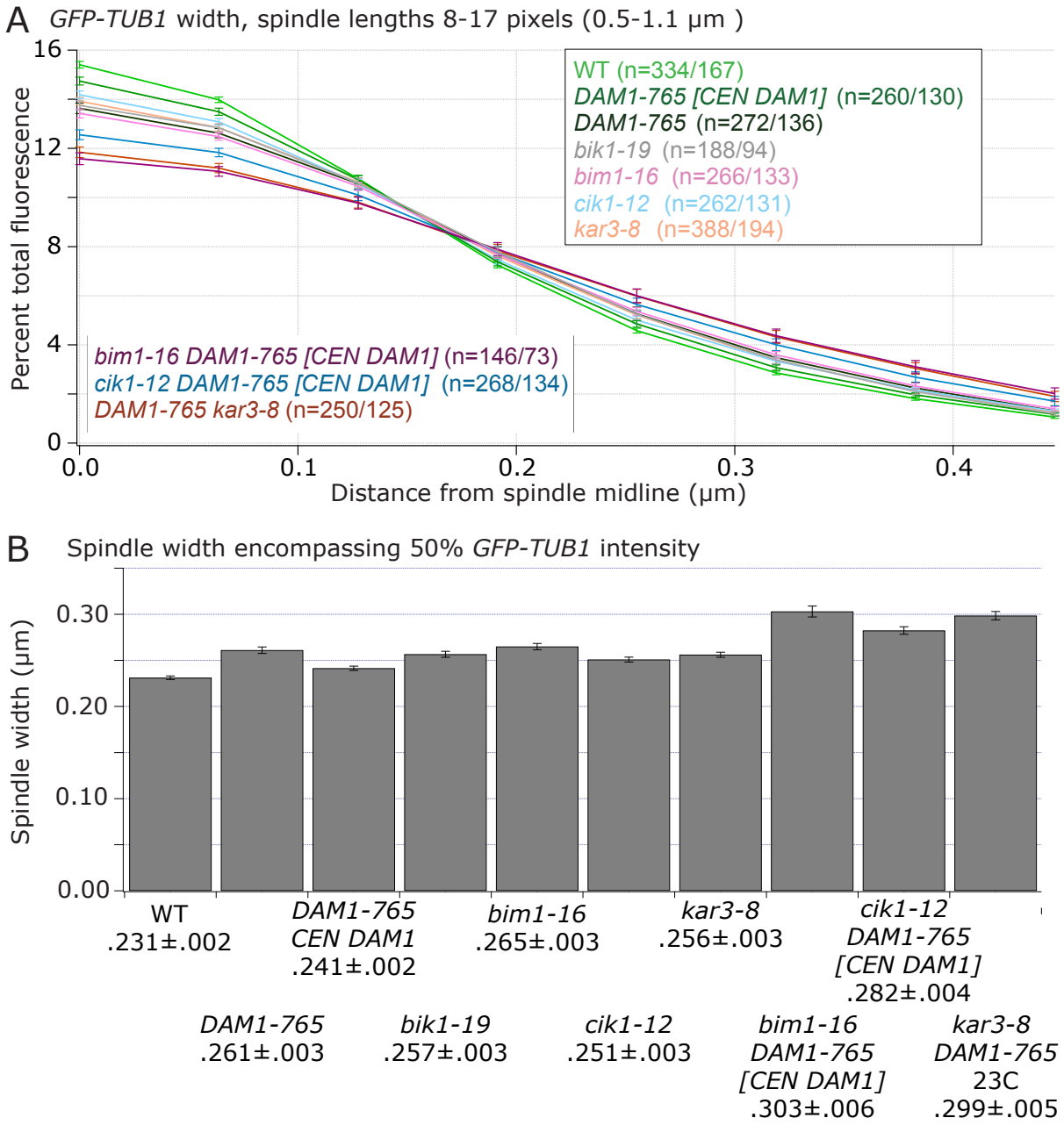

Figure 2.4: Longitudinal *GFP-TUB1* fluorescence in pre-metaphase spindles. A: Cells with fluorescently labeled poles and tubulin were treated as in Figure 2.2. Pre-metaphase spindles (spindles of length 0.5-1.1 µm) were analyzed. *GFP-TUB1* fluorescence was summed along the pole-to-pole midline and along adjacent lines at successively wider 0.638 µm intervals. A: Fluorescence intensity at different widths from the spindle midline. Error bars indicate standard error. The second n value represents the n value of the spindle midline point (0.0), and the first n value represents the n of each other point. Intensity is strongest at the midline and decreases with increased distance. WT *GFP-TUB1* is best concentrated at the spindle midline, single mutant *GFP-TUB1* shows broader fluorescence, and double mutants show a yet broader spread of fluorescence. B. Spindle diameters that encompass 50% of observed spindle *GFP-TUB1*, from the same data set as part A. Again, single mutants show a slightly increased *GFP-TUB1* spread which is increased even more in double mutants.

C

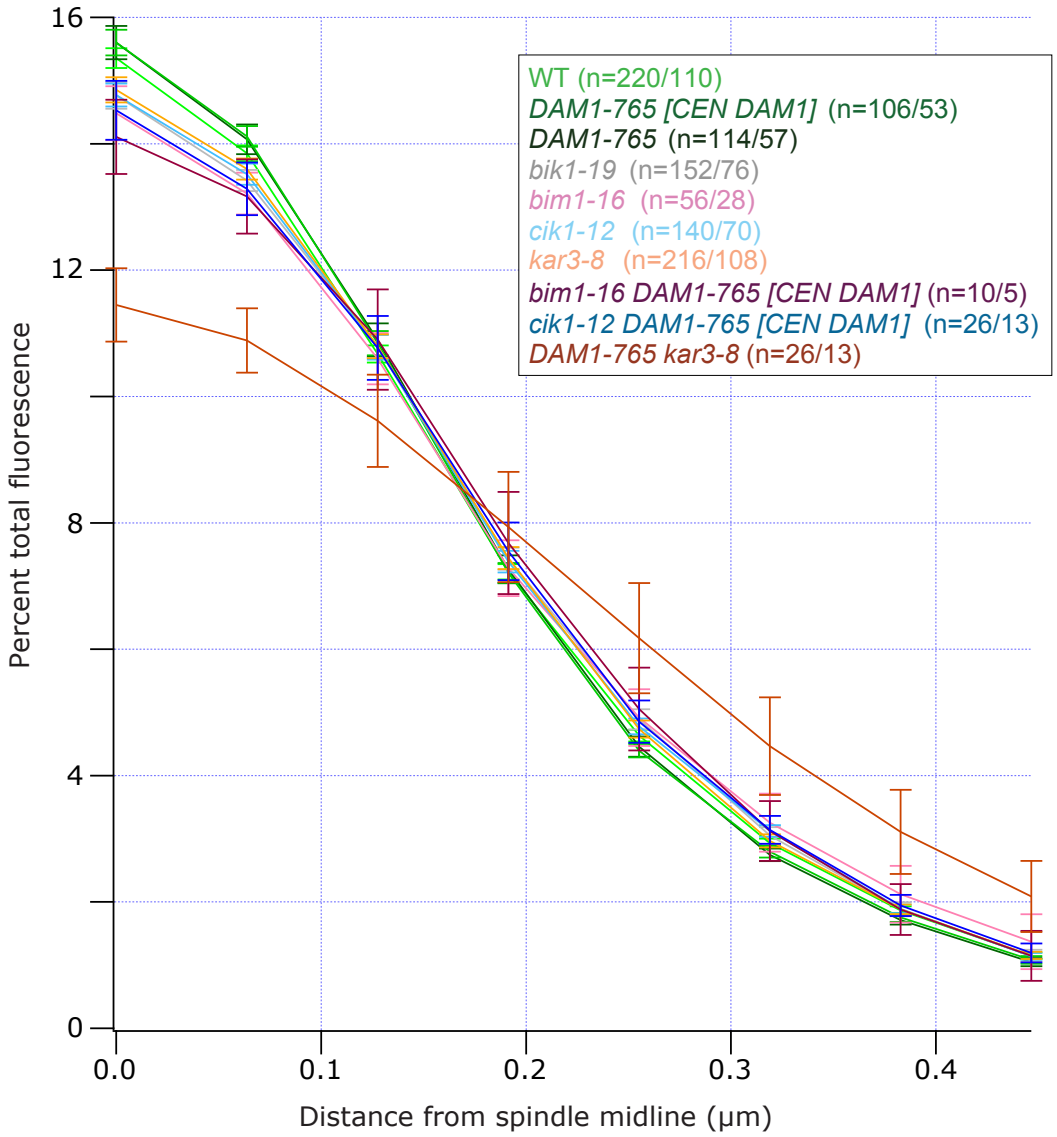

Figure 2.4, continued: C: Longitudinal *GFP-TUB1* fluorescence in metaphase spindles. Spindles of length 1.2-1.5 μm were analyzed using the same method as in Figure 2.4A. Double mutant spindles show more diffuse fluorescence than their single mutant counterparts. With the exception of *DAM1-765 kar3-8*, the difference between single and double mutants is less dramatic than that seen in the shorter spindles in Figure 2.4A.

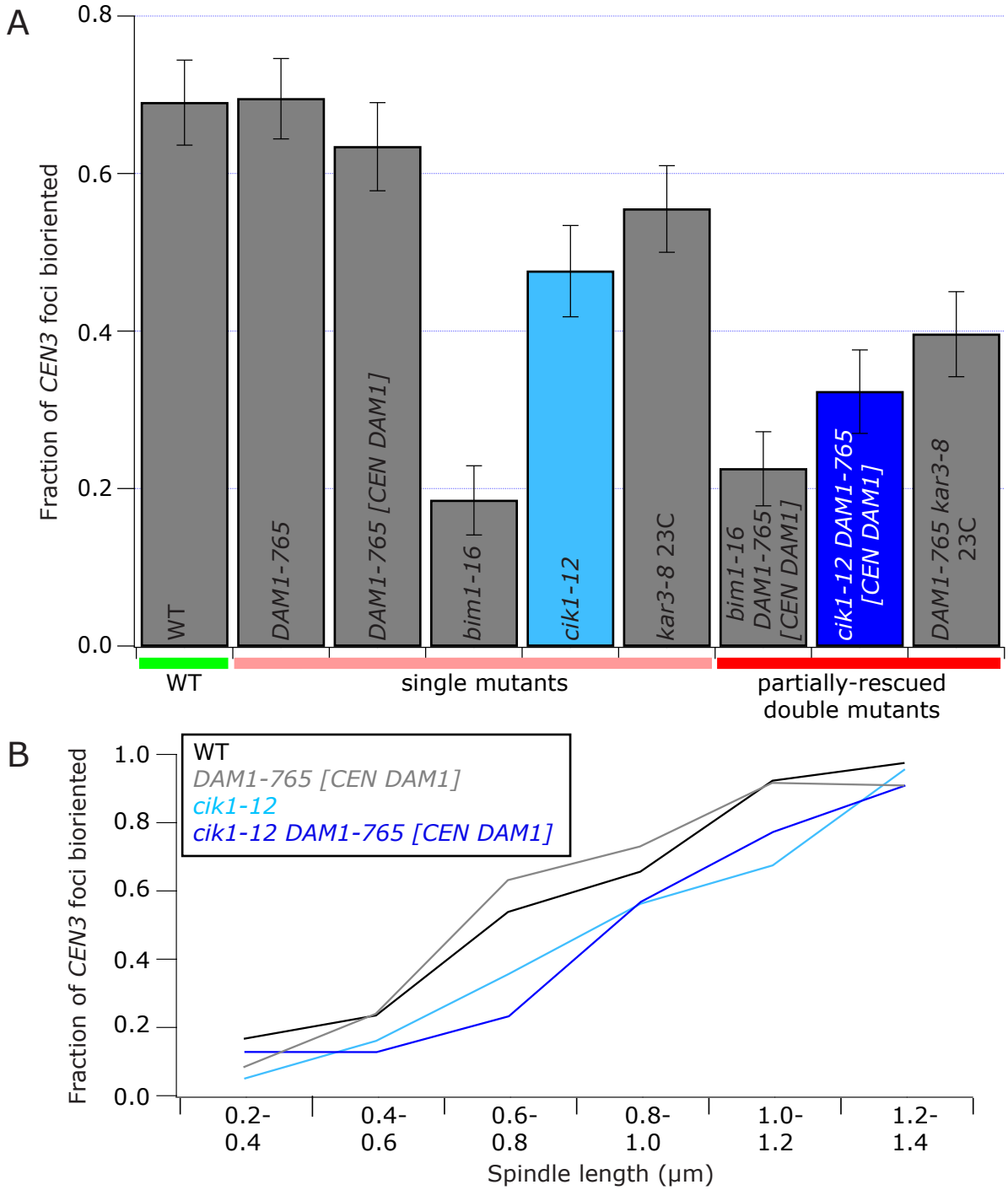

Figure 2.5: GFP-labeled *CEN3* biorientation in various strains. Cells were incubated overnight at room temperature and imaged as described in Materials & Methods. A: Fraction of *CEN3* foci bioriented in pre-anaphase spindles. Though *DAM1-765* biorientation rates are similar to WT, all screen-produced mutations biorient poorly. In *cik1-12* and *kar3-8*, the presence of a *DAM1-765* background further reduces the number of bioriented spindles. B: *CEN3* biorientation rates binned by spindle length. Biorientation frequency increases with spindle length. At any given spindle length, *cik1-12* spindles are more rarely bioriented than WT. No further decrease in biorientation frequency occurs in a *cik1-12 DAM1-765* double mutant, however.

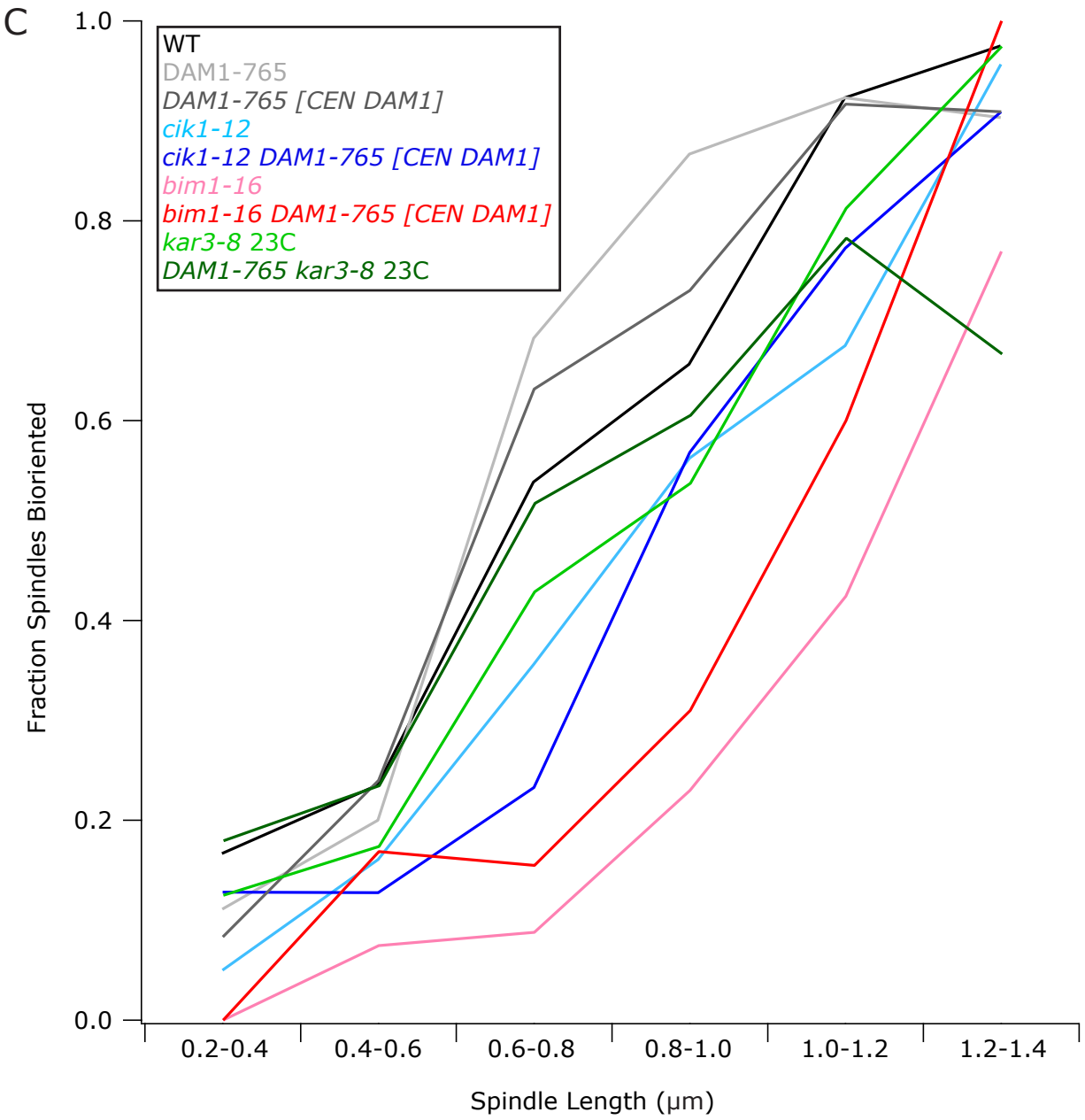

Figure 2.5, continued: C: Additional *CEN3* biorientation data, presented as in Figure 2.5B. Though all screen-produced mutations biorient more poorly than WT, none show a synthetic reduction in biorientation frequency in a *DAM1-765* background.

Chapter III

Cik1 Contains a Conserved SxIP Motif Required for Proper Regulation of Metaphase and Anaphase Microtubules

Introduction

Both Bim1 and Kar3/Cik1 are known to assist in bundling interpolar microtubules (Gardner et al., 2008). It is not immediately clear how they accomplish this task, however. Though both Bim1 (which exists as a homodimer) and Kar3/Cik1 dimers contain two microtubule binding domains each, both dimers are typically thought to bind a single target microtubule (Allingham et al., 2007; Honnappa et al., 2005; Mackey and Gilbert, 2003; Manning et al., 1999). To successfully bundle multiple microtubules, the dimers would need either an additional unknown microtubule-binding site, or an interaction with another microtubule-binding protein. In the case of Kar3/Cik1 homologs, both models have been proposed. Direct binding of kinesin tail regions to microtubules has been speculated to play a role in spindle assembly (Janson et al., 2007; Manning and Snyder, 2000). And the fission yeast EB1 homolog Mal3 is thought to load Klp2 onto spindle microtubules during the final stages of mitosis (Mana-Capelli et al., 2012). Binding of the fly Kar3/Cik1 homolog Ncd to the Bim1 homolog EB1 is thought to assist in bundling K-fibers (Goshima et al., 2005). Though yeast kinetochores attach to single microtubules rather than K-fibers, the notion of an interaction between Bim1 and Kar3/Cik1 is intriguing, since such an interaction would endow both dimers with the potential to bundle interpolar microtubules.

A short sequence motif that EB1 recognizes and binds to, Ser-x-Ile-Pro (SxIP), was recently discovered and found to be widely conserved in animals (Honnappa et al., 2009). This motif is also found at residues 4-7 of Cik1 (personal observation) (see Figure 3.1). Animal SxIP motifs tend to be found in disorganized domains and phosphoregulated by surrounding

serine residues (Honnappa et al., 2009). The N-terminus of Cik1 contains 3 serines in its first 13 residues and is predicted to be disordered via GlobPlot 2 analysis (http://globplot.embl.de/). SxIP motifs also tend to be found in multiples, however, and tend to be in basic environments (Honnappa et al., 2009). The N-terminus of Cik1 is not notably basic, and no further SxIP motifs are found in either Cik1 or Kar3. Despite those drawbacks, I hypothesized that SxIP motifs are conserved from animals to fungi and that binding of Bim1 to Cik1's SxIP motif allows both Bim1 and Kar3/Cik1 to participate in bundling interpolar microtubules.

Results

Cik1 contains an N-terminal SxIP motif that is broadly conserved in kinesin-14s

On a broad level, the amino acid sequences of kinesin-14s are not well conserved between animals and fungi. Cik1 was not identified as a kinesin homolog via analysis of its primary structure; it was only identified as such after the crystal structure of its paralog Vik1 was solved and proved to be similar to kinesin motor domains (Allingham et al., 2007; Manning et al., 1999). I have found, however, that an N-terminal SxIP motif is in fact a widely conserved element of kinesin-14s despite the dissimilarity of the rest of their sequences.

I assembled a collection of sequences of kinesins with C-terminal motors, a defining trait of kinesin-14s (Lawrence et al., 2004), via BLAST searches of known kinesin-14s in the *Saccharomyces* Genome Database, Ensembl.org, *Strongylocentrotus purpuratus* genome database, and the National Center for Biotechnology Information's Protein database. My search yielded sequences from roughly 100 fungal, protist, and animal species that were of similar length to Cik1 and were either annotated as a kinesin-14 or closely homologous to an established kinesin-14. Nearly all species surveyed that had a sequenced C-terminal motor kinesin of similar length to Cik1 possessed a kinesin with a SxIP motif within its N-

terminal 60 residues (see Table 3.1). Some conservative substitutions were apparent; the actual conserved motif is Ser/Thr – x – Ala/Ile/Leu/Val – Pro. These substitutions are similar to those already found in verified SxIP motifs (Honnappa et al., 2009). The sequences surrounding these SxIP motifs are otherwise poorly conserved, as would be expected of a disorganized domain. The extreme conservation of these SxIP motifs suggests that the motif plays a fundamental role in the function of C-terminal kinesins across a broad spectrum of phyla. Interestingly, I did not find that the SxIP motif was conserved in plant kinesin-14s.

cik1-4A reduces Cik1 spindle fluorescence

The Bim1 homolog EB1 is known to recruit cargo proteins to spindle microtubule plus ends (Slep and Vale, 2007). If Cik1's SxIP motif functions as a Bim1 binding site, it could be instrumental in recruiting Kar3/Cik1 to the mitotic spindle. To determine whether Cik1's SxIP motif is necessary for spindle localization of Cik1 or Bim1, I constructed two alleles of Cik1, *cik1-4A* and *cik1-4A-GFP,* that have their SxIP motifs mutated to four alanine residues. I then assayed the spindle fluorescence intensity of *BIM1-CFP* in wild-type and *cik1-4A* backgrounds, and also compared *cik1-4A-GFP*'s intensity to that of *CIK1-GFP* (see Figure 3.2). *cik1-4A* does not significantly alter *BIM1-CFP* fluorescence. *cik1-4A-GFP* is 43% dimmer than *CIK1-GFP* ($p<0.0005$). These results demonstrate that Cik1's SxIP motif is necessary for full spindle recruitment of Cik1 but is not necessary for Bim1 recruitment. By extension, it suggests that Bim1 may recruit Kar3/Cik1 to the spindle, but not vice versa.

cik1-4A-GFP metaphase and anaphase spindles are shorter than wild-type

To determine what effect mutating Cik1's SxIP motif has on interpolar microtubules, I measured interpolar distances in asynchronous cells in *CIK1-GFP* and *cik1-4A-GFP* backgrounds and found a striking defect in anaphase spindle elongation. While *CIK1-GFP*

anaphase spindles frequently extend up to 7-9 μm in length, *cik1-4A-GFP* spindles dramatically slow down anaphase elongation at roughly 2.5 μm and rarely surpass 5 μm (see Figure 3.3). Interestingly, *bim1-16* suppresses the anaphase length defect. *cik1-4A-GFP* pre-anaphase spindles are also shorter than WT (see Figure 3.3).

Though both *cik1-12* and *cik1-4A-GFP* mutate Cik1's N-terminus, they display very different phenotypes. The spindle length defects seen in *cik1-4A-GFP* are specific to that allele and are not found in *cik1-12* (see Figure 2.2). *cik1-4A-GFP* is synthetically sick with *DAM1-765,* and that sickness correlates with a further reduced pre-anaphase spindle length (see Figure 3.3), but it is not synthetically lethal.

To confirm the phenotypes observed in *cik1-4A-GFP*, I measured spindle lengths of a *cik1-4A* strain that lacks a GFP tag on Cik1. Surprisingly, the anaphase defect seen in *cik1-4A-GFP* is not present in *cik1-4A*. *cik1-4A* is also healthy in conjunction with *DAM1-765*. *cik1-4A DAM1-765* cells still accumulate at a shorter preanaphase length, however (see Figure 3.3). Mutation of Cik1's SxIP motif therefore triggers anaphase length defects only in the presence of a GFP tag on Cik1.

Cik1's SxIP motif is not sufficient to drive spindle localization

To determine whether Cik1's SxIP motif is sufficient to recruit proteins to microtubule plus ends, I fused the N-terminal portion of Cik1 to GFP and expressed the construct on an autonomous plasmid under control of the yeast calmodulin promoter. A similar approach was used to originally characterize SxIP motifs in animal cells (Honnappa et al., 2009). I used two constructs containing different amounts of Cik1's N-terminus. The first (shorter) construct contained Cik1 residues 1-13, while the second construct contained residues 1-34. This second construct was long enough to include Cik1's putative nuclear localization signal

(residues 24-33), but stopped short of Cik1's alternative start codon (residue 35) (Benanti et al., 2009; Manning et al., 1999) (see Figure 3.1).

Cells containing the shorter construct displayed diffuse fluorescence throughout the cell (see Figure 3.4). Cells containing the longer construct displayed diffuse fluorescence that was concentrated inside an intracellular compartment, presumably the nucleus (see Figure 3.4). These results confirm the presence of a nuclear localization signal between residues 14 and 34 of Cik1, but also demonstrate that Cik1's SxIP motif is not sufficient to recruit GFP to the mitotic spindle. My results do not rule out an association between Cik1 and Bim1 via Cik1's SxIP motif. Bim1 binding is typically driven by more than one SxIP motif (Honnappa et al., 2009), and there may be one or more cryptic Bim1-binding motifs on Cik1 or Kar3 that are necessary for strong association with Bim1.

Discussion

Similar suites of interpolar microtubule-bundling & regulating proteins, including Ase1, Cin8, Kip1, Bim1, and Kar3/Cik1, are present on interpolar microtubules both before and after the onset of anaphase (Gardner et al., 2008; Janson et al., 2007; Kotwaliwale et al., 2007; Straight et al., 1998). But though similar sets of proteins are involved in each phase, their roles shift before and after anaphase onset. Cin8 and Kip1 appear to be largely redundant before anaphase, for example (Hoyt et al., 1992; Saunders and Hoyt, 1992), but after anaphase they segregate roles: Cin8 drives anaphase extension in the initial fast phase of anaphase B, and Kip1 drives extension in anaphase B's subsequent slow phase (Straight et al., 1998). The stark difference in phenotype of *cik1-12* and *cik1-4A*, which each impact a different phase of mitosis, suggests that Cik1 may also switch roles between phases. *cik1-12*'s clearest impact is on pre-anaphase ipMT bundling, length regulation, and biorientation

(see Figures 2.2, 2.4 and 2.5). *cik1-4A* is comparatively mild during those steps, but instead generates a striking anaphase elongation defect.

In my spindle length results, the transition from anaphase B phase one to the slightly slower-extending phase two appears to take place in wild-type cells at a spindle length of roughly 4.2-4.5 μm (see Figures 2.2 & 3.3). *cik1-4A-GFP* anaphase B also has two clear sub-phases: a fast phase from 1.0-2.5 μm in spindle length and a slow phase from 2.5-4.5 μm (see Figure 3.3). The *cik1-4A-GFP* subphases could be the classic phase one and phase two happening at abnormally short spindle lengths. Two features of the results, however, suggest that the *cik1-4A-GFP* subphases may instead represent phase one spindles that slow and stop as phase two fails to engage. *cik1-4A-GFP* spindles stop extending at roughly the same spindle length (4.5 μm) at which phase 2 normally begins. Furthermore, the change in elongation rate between *cik1-4A-GFP* anaphase subphases is much more pronounced than the change in rate between wild-type phases one and two. If *cik1-4A-GFP*'s second subphase is a true phase two, it is impacted by Cik1 mutation far more than phase one.

I can confidently conclude, however, that *cik1-4A-GFP* has an anaphase elongation defect that is definitely at play during anaphase B phase 2 and that may be active during phase 1 as well. The anaphase length phenotype is consistent with a defect in regulation of microtubule length, microtubule overlap, or both, and the defect may be specific to mutation in Cik1's Bim1-binding motif. My results provide further evidence for a widely conserved interaction between EB1 homologs and kinesin-14s.

Materials & Methods

Cloning

cik1-4A was made using the Delitto Perfetto approach (Storici and Resnick, 2006) and verified via sequencing.

cik1-4A-GFP was made via PCR of *CIK1-GFP::KanMX* using primers that replaced the SxIP motif with alanine residues, followed by transformation of the PCR product into a *cik1Δ* strain. The allele was then verified via sequencing.

SKIP-GFP vectors were made by modifying the GFP sequence on pFA6 S65T (available from the Yeast Resource Center) to remove NcoI and BamHI sites using Agilent Technologies' QuikChange Site-Directed Mutagenesis system. The N-terminal portion of Cik1 preceded by an NcoI site was added to the N-terminus of GFP and a BamHI site was added to GFP's C-terminus via PCR, and this cassette was ligated into the NcoI-BamHI fragment of pJG7 (Geiser et al., 1991), placing *SxIP-GFP* under the control of pJG7's yeast calmodulin promoter.

Microscopy

Microscopy, fluorescence intensity measurements, and spindle length measurements were performed as described in Chapter II.

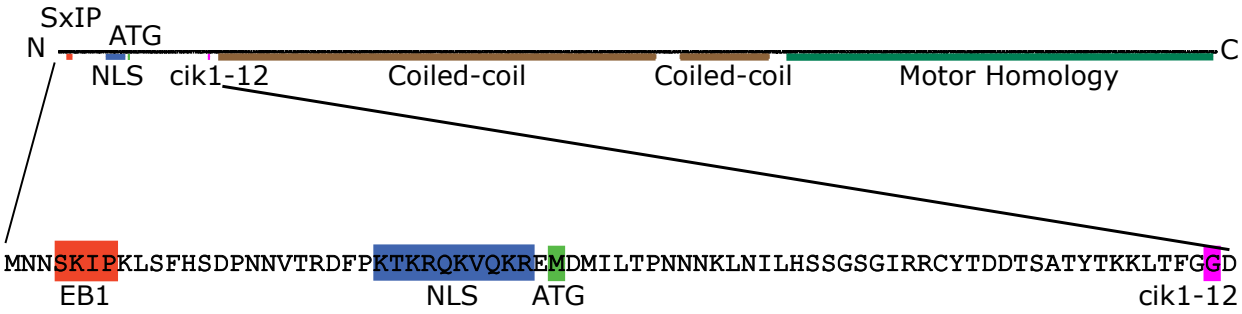

Figure 3.1: Domain structure of Cik1. Cik1's N-terminus contains a SxIP motif, followed by a putative nuclear localization signal, an alternate start codon, and the locus of the *cik1-12* mutation. The N-terminus is followed by a pair of coiled-coil domains used in dimerization with Kar3 and a C-terminal motor homology domain (Benanti et al., 2009; Manning et al., 1999).

Table 3.1: List of 70 species with kinesins containing the motif S/T-x-A/I/L/V-P

Species	Common name	Protein name	Genbank/Ensembl ID	first 70 AA
Saccharomyces cerevisiae	budding yeast	Cik1	CAA87820.1	MNN**SKIP**KLSFHSDPNNVTRDFPKT KRQKVQKREMDMILTPNNNKLNILH SSGSGIRRCYTDDTSATYTK
Saccharomyces kudriavzevii	(ascomycota)	Cik1-like protein	EJT42048.1	MNN**SKIP**KLSLHSDHSGNTRDTFKN KRQKVQKKEMDMVLTPNNNKLNILQ GSRSGIRRCFTDDPSAVNKK
Saccharomyces arboricola	(ascomycota)	cik1p	EJS44163.1	MNN**SKIP**KLSFHSDSNSNTRDFSRI KRQKLQKGEMDMVLTPNNNKLNILQ SSGAGVRRCFTDDSSIMQKR
Zygosaccharomyces rouxii	(ascomycota)	ZYRO0C05676p	CAR26969.1	MNH**SKIP**SISTSGANLSIKRRRLSS SPMLQDVTNHVYTRPSIRHVSEGHS QQQNRRLLNKYIYGDATVIE
Lachancea thermotolerans	(ascomycota)	KLTH0A05544p	XP_002551699.1	MTH**TKIP**QMSQ**TRIP**GHKRAMSSPP GSATKRLHILEDVTNTNSIARLPGT KMSVAVDSNTRLMNKYYYGD
Ashbya gossypii	(ascomycota)	AFL170Cp	NP_985380.1	MNK**TRIP**SISLKRARECGEVDSQPP RYKRASGKSPLAEITNTASSSPHIS EDKMLSTKSMFGSSGQSSRL
Kluyveromyces lactis	(ascomycota)	KLLA0B10329p	CAH02382.1	MNE**TRIP**SINSRKRQKPFSSGSVSG QKKHHPVLANITNMVTTTGTTTVAN SSGSKKEQFAPSYQTKSQST
Naumovozyma dairenensis	(ascomycota)	NDAI_0I00650	XP_003671877.1	MSNQ**SRIP**FLSYNHTTINNNNNNNN TRQNNKIEPPVYKKPKLSM**SPIP**RS PMLKDVTNHFNSHTTMSSSR

Table 3.1, continued

Naumovozyma castellii	(ascomycota)	hypothetical protein	XP_003676371.1	MHNN**SRIP**SL**SSLP**PVNKKPKLSSP IPMSTTLKDVTNKMIGIPTESMTTP TYNNKLTYGNDDLMETFKKR
Aspergillus nidulans	(ascomycota)	KLPA	XP_663944.1	MQG**SRIP**GLKEMNPSGTNAR**SRLP**Q PGAIANKPTAVPQLARTRSTTESTR IGAGPPSAARSVNGATKAHT
Yarrowia lipolytica	(ascomycota)	YALI0C12859p	XP_501776.1	MDNVLQPHKGAN**SGIP**RFVAKSAKV SEHKPRSVANNENVPIGSKRPAPGA LPVPVSRLHKDDTLYGRRTG
Candida albicans	(ascomycota)	KAR3	AAN85373.1	MSDENTKHKFLNVSQPSNLLGGSSS SNSLRRPLNDNTVSVSNKMRKTT**SQ IP**VAKDTVPTLTISESNRFR
Aspergillus fumigatus	(ascomycota)	KlpA	XP_755761.1	MAGMTSGMTNSR**SGLP**QPGTIASKT SSLSHTTRARSA**TQAP**EPSRSGTGS LPPSRPGTSMGRVHTRTNSH
Vanderwaltozyma polyspora	(ascomycota)	hypothetical protein	XP_001647353.1	MSN**SKIP**SLSSTPSAPNSYPRLKRA RLSLGNSMLHDVTNNVNNRLVSRRS LAGNISTATTTSSSSQSMRL
Schizosaccharomyces pombe	fission yeast	Klp2	CAB65811.1	MEEEGHKSLT**SHLP**QSSSSLSQSRE IAKEFT**SNIP**PPTIKTNSSSSNILK PRLSLQNEVNQLKPAKFPSK
Fibroporia radiculosa	(basidiomycota)	predicted protein	CCM01834.1	M**SRLP**RLHPSSSPDRHQSGPSMSFS TRQGSLKRKAQDENFNIAEQQPRKL AAIAEADTNQPLRPSKAAIS

Table 3.1, continued

Tremella mesenterica	(basidiomycota)	hypothetical protein	EIW66111.1	M**STLP**LLTANNANKRKTPSSPAGPA AKRQASASSLGKSTSGPKKPPGFIP TTTRKPSGTLSRPTSSLSTS
Cryptococcus neoformans	(basidiomycota)	kinesin	XP_571545.1	MEQENNPPPL**SRLP**RLASPIKP**SSI** **P**VPSAA**SSIP**HMPPLTSDNNANTGI SKRKMPSSPMHPPVAKRSVS
Entamoeba histolytica	amoeba	kinesin	XP_651474.1	MSLPHSDDLYKHVAQPPPDF**SKVP**P LFRSTPLIRHHNASKPRLIKESTIT KPQNNTKHSSLKLSSSKPIP
Naegleria gruberi	protist	kinesin-14	EFC46509.1	MSTLTPNNYLKRKRSDENSPTDQEN VNPNKKT**SKIP**VLKHSNSSSSLNSS TLSTNKTTPVKPTLPTRTNS
Giardia lamblia	protist	kinesin-14	EFO61004.1	MDDRLQFTIIHVAERRKFKITVRVE DVPNVRVRMLKKSIFQA**TGIP**VDCQ ALYLNKQLLSDRMTGSELKL
Caenorhabditis elegans	nematode	KLP-15	CCD71345.1	MNVARRRSGLFRSTIGATPKITRGR AAAPSTKEANS**TTIP**RQSAPGGITI GAAARRPP**SRLP**TPTTPATG
Trichinella spiralis	nematode	putative kinesin motor domain protein	XP_003376424.1	MYHVELARELPMRLM**SRIP**KAVSTG IVKDHSNDTKLSEKSLIATPAKSVL TSKTKAVNPPRKALPTAVRK
Apis mellifera	honeybee	protein claret segregational	XP_001122238.2	ME**SRLP**KPKFNLSKVVSTENIKTNN QKMPKYQNDLPDASSNHVSDKLKKT KSTINITAKCRNENKPPAKQ

Table 3.1, continued

Pediculus humanus corporis	lice	protein claret segregational	XP_002424355.1	MDPGHFLTNSG**SKIP**MPKSKKENII PSRPKLAPSAVTTTNYLGEKANNYS ENKESVPNIAKSSVGITRCK
Eriocheir sinensis	crab	KIFC1	ADJ19048.1	M**SKLP**SSASRHLHQPSRLRPPGSAM KRLGSDSAITSPQKKTRHSGDAEDT GAMARSQRLGGPRAAPGLSR
Drosophila melanogaster	fly	non-claret disjunctional	NP_476651.1	ME**SRLP**KPSGLKKPQMPIK**TVLP**TD RIRAGLGGGAAGAGAFNVNANQTYC GNLLPPLSRDLNNLPQVLER
Drosophila pseudoobscura pseudoobscura	fly	GA20615	XP_001358980.2	ME**SRLP**KPTSIKRPMMPVK**SILP**TD RIKAGGQGGAFSANQTYCGNLLPPL SRDINNLQEMDRRRGRAASP
Harpegnathos saltator	ant	protein claret segregational	EFN76819.1	ME**SRLP**KPKIIVKKTINTMDINTNN KQQAVKSGENAVKPTSTKTTNETKP LPKPLLVRSKTLTTFTRTNN
Camponotus floridanus	ant	protein claret segregational	EFN66508.1	ME**SRLP**RPKVTLTKAISTMEVNIKS ISNKIAKEENNIPASVSNAKSTATS SFASKSTYPIKENKPPTLVR
Bombyx mori	silkworm	Ncd	NP_001119723.1	M**SKIP**KLPTISKENRFGQFHNRPIS RTIANGLSDVDKKNLITNHTRPLRN GPPVSAAAPRIKRSATAPSS
Danaus plexippus	monarch butterfly	Ncd	EHJ73962.1	M**SRIP**KYPVSAAKENRPGISNSRII SRTIGNGFSDVEKKNLLMNHTKPMN GTTTNKVAAPRIKRSATAPS

Table 3.1, continued

Anopheles darlingi	mosquito	AND_02359	EFR29016.1	MD**SKIP**KPSFLKKPAAISTLSLPGN ARLPLSRDLLNVPSAINSTMFGMLK ARAASPELRSENYGAGRPEI
Octopus tankahkeei	octopus	KIFC1-like kinesin	ADI48081.1	MNGQRKVLADTANCS**SKLP**KLTPKL AKRKNSPNETEQVKKMRFQKPVSKI RTNLAPSSRLVNSQSIAGYN
Aplysia californica	sea hare	C-terminal kinesin-2-like isoform X1	XP_005102126.1	MDSSRKPLATRSNL**SRLP**LPGSRQK RARSPEDEVVNVPSGGKKSRLEVPP PNQTTKPARSLSSSTLTAAR
Strongylocentrotus purpuratus	urchin	Sp-KifC1	*Sp* genome SPU_017289	MSYFFVPQRASAIDQRGMHGARSLL TTQQQVEKSFILQPC**TLVP**NISMSR QGSALSEQDPNVIRRGVSKL
Ciona intestinalis	sea squirt	kinesin family member C1-like-like	XP_002120068.1	MDVSV**SKLP**QK**SKLP**APMNRSLFGA NSSHLQSPRTYSLQSRLNKENNAPK PKVTFETDCAEMRMAKRKSE
Danio rerio	zebrafish	kinesin family member C1 isoform X1	XP_005159465.1	MNKENT**SRLP**VMSGKRAHTNSTDGE QQQPAQKKMRKVEVEPSQRFRPAA**S** **VAP**PRRPVAVKAPVKPLRPT
Oryzias latipes	medaka	carboxy-terminal kinesin 2-like	XP_004074113.1	M**SRLP**VMTSKRVLTNSNSENAQVMA PAQKKMRREQDMHKPQAAATVIGHR QAPVAA**SRAP**HSESIRTAGA
Salmo salar	salmon	kinesin family member C1	ABO13867.1	MNKENT**SRLP**VMSGKRVLSASSSES INSCSDQQPAQKKMRRVDSDPKMRQ TASAMGTKRPLPPKRAVAAK

Table 3.1, continued

Gasterosteus aculeatus	stickleback	KIFC1	ENSGACG00000001865	M**SRLP**VSASKRVLLTSSSSSENGQD FAPAQKKIRKDPEPFKPHAAATIIS GRRPPVAA**TRAP**ISRPVRGV
Latimeria chalumnae	coelacanth	KIFC1	ENSLACG00000006938	MSEKVS**SRLP**VLKLGKKVLREENQQ QRSLKRQCDTSPGHDLPKKKMVVSV VLKQSQAMAPIPRNPRGAGG
Andrius davidianus	salamander	kinesin-like motor protein	AEB71794.1	MNVNENKPLAAVKAV**SRLP**VPSTVR PKRSRSSENMPLIEKKRIRISSPEQ HAVRRSVPASIATTRPKPPV
Xenopus laevis	frog	carboxy-terminal kinesin 2	NP_001081003.1	MDSTDKKVQVA**SRLP**VPPKRKYVSN DENQEQMQRKRLRSSLE**SELP**AVRV AASIATSKPRAAPVAALPKP
Chelonia midas	sea turtle	carboxy-terminal kinesin 2	EMP26575.1	MEQKGNADGRQVPLAGKAL**SQLP**VP GLRAKRGHSDENQPPTEQKRARRLP VPTRRVAASIATTCSKASAA
Gallus gallus	chicken	carboxy-terminal kinesin 1	BAF62975.1	MAAVGSGGSVGAAPGMAVVAPLPAP T**SRLP**VRRAAAKRAASGPQPAAPEQ KRARSGTASSQPPGRAPLWA
Monodelphis domestica	opossum	KIFC1	XP_001377667.2	MASCFLQKLSRMEKDNMELKMPPDK ASS**SQLP**VLGLSAKRGLDKENVPEP KKKRARGPGTAATIAISHPR
Sarcophilus harrisii	tasmanian devil	kinesin-like protein KIFC1	XP_003769017.1	MEKGSKELKMPSDKASS**SRLP**VLGL GRKRRLDKENAPEPEKKRIRGTG**TT IP**MSCLKEATVATIPRAKKQ

Table 3.1, continued

Orcinus orca	orca	kinesin-like protein KIFC1 isoform 1	XP_004267780.1	MEPQRSPLLEVKGNIELKRALAKAP **SRLP**LPGSRLKRGPDQMEEDLEPEK KRKRGLGTKVATSRPRATAL
Canis lupus familiaris	dog	kinesin family member C1	XP_849869.2	MEPQRSPLLEVRGNIELKRPLVKAP **SRLP**LPGTRFKRGPDQMEDALEPEK KRTRGLDTVTKIATSQ**SRAP**
Equus caballus	horse	kinesin family member C1	XP_001493528.3	MEPQRSPLLEVKGNIEVKRPLVKAP **SRLP**LPGSRFKRGPDQMEDALEPEK KRTRGLGTALKIATSRPRAP
Bos taurus	cow	KIFC1	NP_001095406.1	MEPQRSPLLEVKGNVELKRPLAKAA **SRLP**LSGRRLKRGPDQMEEALEPEK KRTRGLGTRVTTTHPRAAAL
Condylura cristata	mole	KIFC1	XP_004673435.1	MDPQPRSPLLEVKGNVELKRPLVKA P**SRLP**LSGHRLKRGPSQMEDALEPE KKRTRGLGTTIRTATSRPRA
Myotis davidii	bat	KIFC1	ELK26118.1	MEDVLEPEKKRTRGLGTATKFATSH HRAPVIATVPQTQGH**TAAP**KVPKKT GPRCATAVATVLKTQKAGPA
Mus musculus	mouse	KIFC1	NP_001182227.1	MDVQAQRPPLLEVKRNVELKAALVK SS**SRVP**LSASRLKRGPDQMEDALEP AKKRTRVMGAVTKVDTSRPR
Macaca mulatta	rhesus	kinesin family member C1	XP_001109683.1	QKVSKKTGPRCSTAIATGLKNQKPV PAVPVQKPGT**SAVP**PMAGGKKPSKR PAWDLKGQLCDLNAELKRCR

Table 3.1, continued

Papio anubis	baboon	KIFC1	XP_003897497.1	MDPQRSPLLEVKGNIELKRPRIKAP **SRLP**LSGSRLKRRPDQMEDGLEPEK KRTRGLGATTKITTSHPRVP
Gorilla gorilla	gorilla	KIFC1	XP_004043864.1	MDPQRSPLLEVKGNIELKRPLIKTP **SRLP**LSGSRLKRRPDQMEDGLEPEK KRTRGLGATTKITTSHPRVP
Pan troglodytes	chimpanzee	KIFC1	XP_518406.4	MDPQRSPLLEVKGNIELKRPLIKAP **SQLP**LSGSRLKRRPDQMEDGLEPEK KRTRGLGATTKITTSHPRVP
Homo sapiens	human	KIFC1	NP_002254.2	MDPQRSPLLEVKGNIELKRPLIKAP **SQLP**LSGSRLKRRPDQMEDGLEPEK KRTRGLGATTKITTSHPRVP

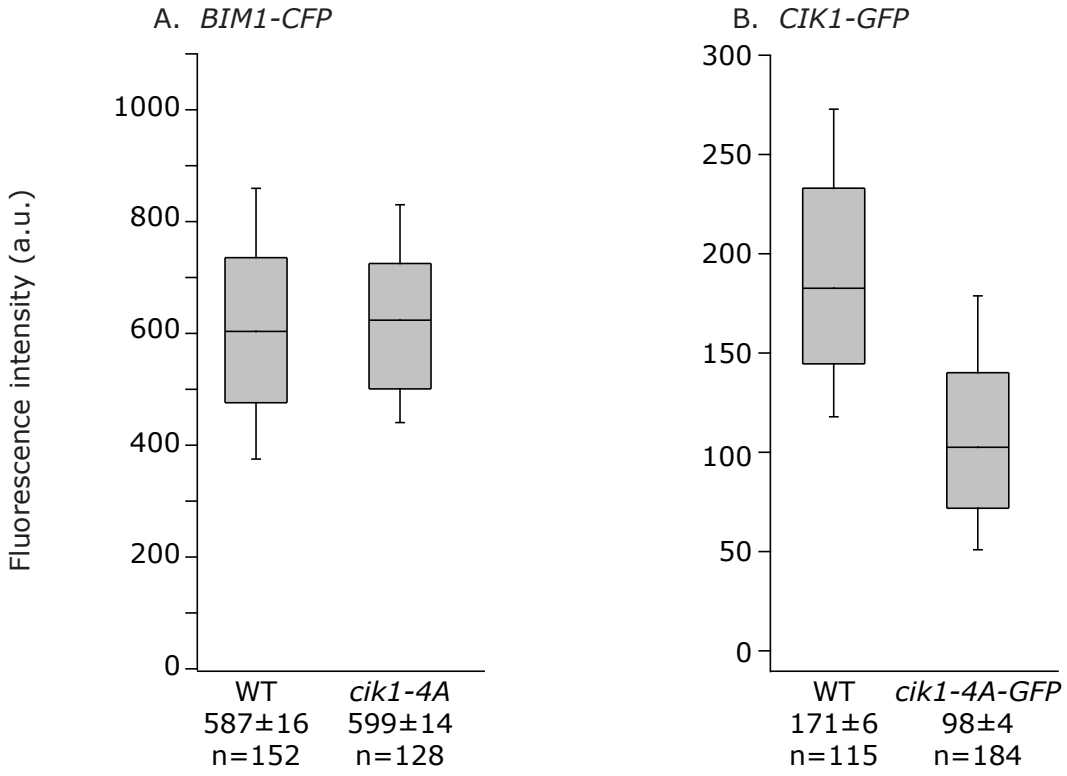

Figure 3.2. Metaphase spindle fluorescence of *BIM1-CFP* and *CIK1-GFP* in WT and *cik1-4A* backgrounds. Cells were treated and data analyzed as in Figure 2.1. Box plots indicate the 10th, 25th, 50th, 75th, and 90th percentiles as in Figure 2.1. X-axes display the genetic background, mean ± standard error as judged by Gaussian fit (arbitrary units), and n value. A: Intensity of BIM1-CFP. Fluorescence is relatively tolerant of Cik1 mutation. B: Intensity of CIK1-GFP. Cik1 fluorescence is reduced by nearly half in *cik1-4A-GFP*.

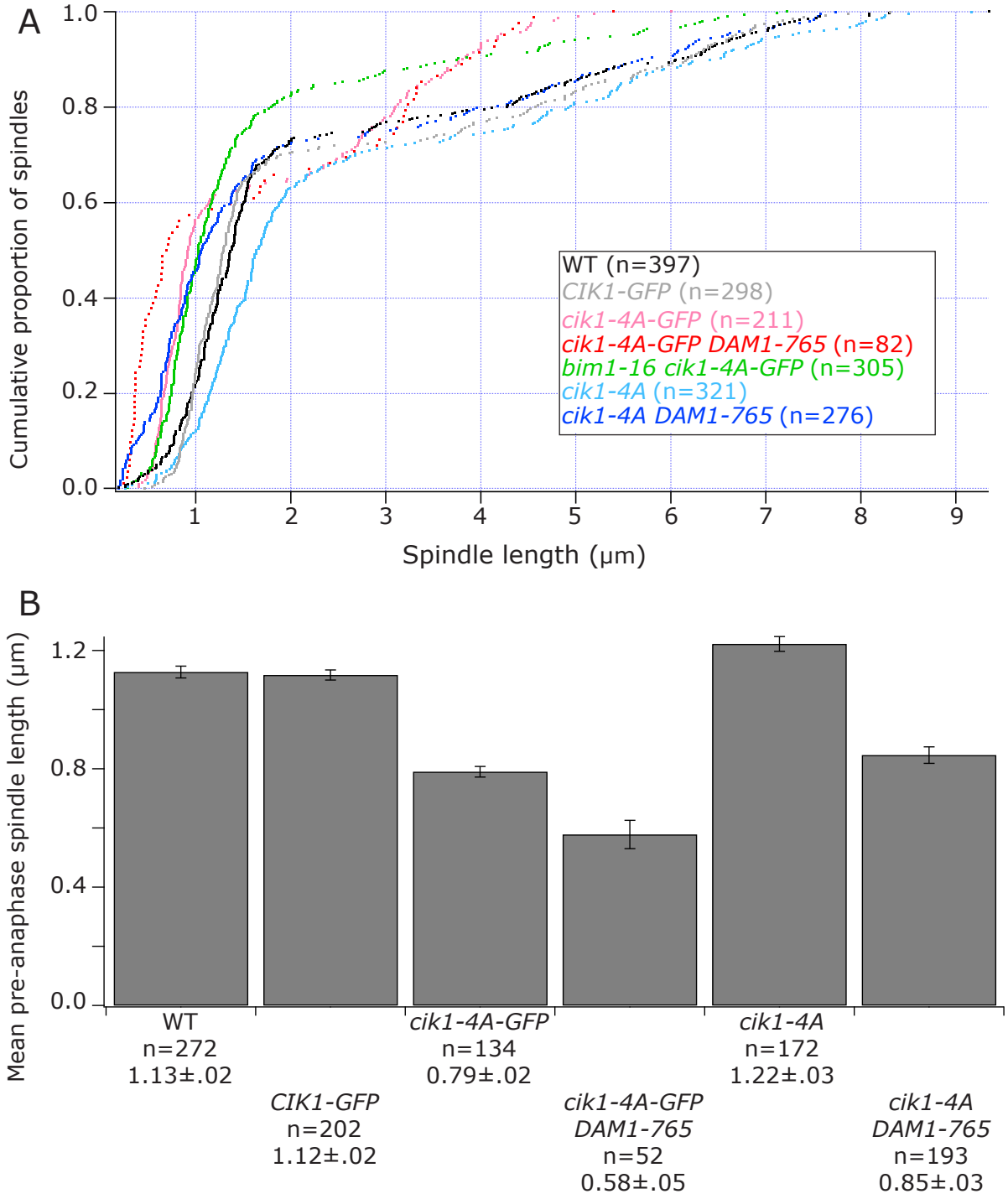

Figure 3.3: Spindle lengths of Cik1 SxIP mutants in asynchronous culture. Data collected and analyzed as in Figure 2.2. A: Anaphase *cik1-4A-GFP* cells slow extension sharply at roughly 2.5 μm in spindle length and rarely surpass 5 μm. This defect remains in a *DAM1-765* background but is suppressed in a *bim1-16* background. Both *CIK1-GFP* cells and *cik1-4A* cells extend to a normal wild-type anaphase length. B: *cik1-4A-GFP* cells accumulate at short pre-anaphase lengths. This defect is not seen in *CIK1-GFP* cells or *cik1-4A* cells, though a *DAM1-765* background results in a synthetic spindle shortening in both Cik1 SxIP mutants (see Figure 2.2 for *DAM1-765* control).

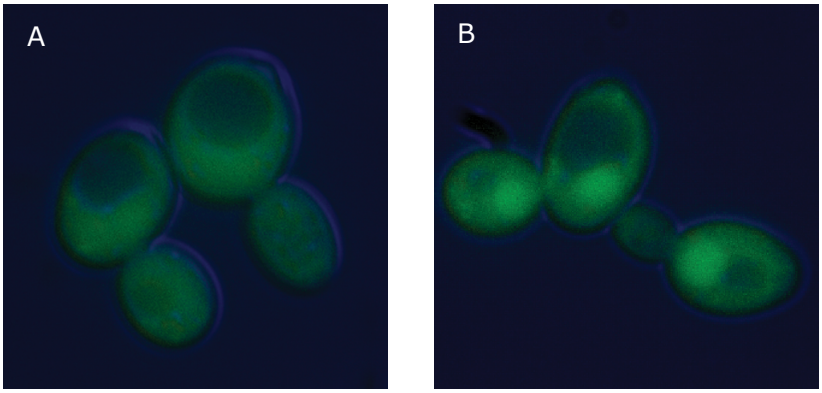

Figure 3.4: *SKIP-GFP* fusions. A: *cik1(aa2-13)-GFP*. B: *cik1(aa2-34)-GFP*. The fusion construct containing the shorter motif is found cell-wide, while the construct with the longer motif including the putative NLS is concentrated in the nucleus.

Table 3.2: Yeast Strains and Plasmids

Strain	Genotype*	Source
EDY60	a DAM1-765::natMX TRP1 pED2	This study
EDY192-2B	@ bim1-16-CFP::KanMX TRP1	This study
EDY167-10D	a CIK1-GFP::KanMX LEU2 LYS2 SPC110-Cherry::hphMX	This study
EDY190-1D	α ADE3 cik1-4A-GFP::KanMX LYS2 SPC110-Cherry::hphMX	This study
MSY112-4D	a BIK1-GFP::TRP1 LYS2 or lys2Δ::HIS3 SPC110-Cherry::hphMX URA3	Michelle Shimogawa
EDY237-1D	a BIK1-GFP::TRP1 cik1-12 LYS2 SPC110-Cherry::hphMX	This study
EDY238-4B	a BIK1-GFP::TRP1 bim1-16 LYS2 SPC110-Cherry::hphMX	This study
EDY239-9C	a BIK1-GFP::TRP1 cik1-4A HIS3 or his3-11,15 LYS2 SPC110-Cherry::hphMX TRP1 URA3	This study
EDY154-4C	a BIM1-CFP::KanMX LYS2 SPC110-Cherry::hphMX TRP1	This study
EDY240-13D	α bik1-19 BIM1-CFP::KanMX SPC110-Cherry::hphMX TRP1	This study
EDY241-1A	α BIM1-CFP::KanMX cik1-12 LYS2 SPC110-Cherry::hphMX	This study
EDY232-5A	a BIM1-CFP::KanMX cik1-4A HIS3 or his3-11,15 LYS2 SPC110-Cherry::hphMX TRP1	This study
EDY242-2B	a bik1-19 CIK1-GFP::KanMX SPC110-Cherry::hphMX TRP1	This study
EDY243-4D	α bim1-16 CIK1-GFP::KanMX LYS2 SPC110-Cherry::hphMX	This study
EDY111-1A	α kar3-8 LYS2 SPC110-Cherry::hphMX GFP-TUB1::LEU2	This study
EDY111-5B	α DAM1-765::natMX LYS2 SPC110-Cherry::hphMX GFP-TUB1::LEU2	This study
EDY111-6B	a DAM1-765::natMX kar3-8 LYS2 SPC110-Cherry::hphMX GFP-TUB1::LEU2	This study
KFY11-3A	a GFP-TUB1::LEU2 SPC110-Cherry::hphMX	Kim Fong
EDY169-8C	a bim1-16 GFP-TUB1::LEU2 NUF2-Cherry::hphMX SPC110-CFP::KanMX TRP1	This study
EDY160-4C	α cik1-12 GFP-TUB1::LEU2 LYS2 NUF2-Cherry::hphMX SPC110-CFP::KanMX TRP1	This study
EDY122-2B	α cik1-12 DAM1-765::natMX GFP-TUB1::LEU2 LYS2 SPC110-Cherry::hphMX TRP1 pJT11	This study
EDY122-7A	a DAM1-765::natMX GFP-TUB1::LEU2 LYS2 SPC110-Cherry::hphMX pJT11	This study
EDY260-4A	a bim1-16 DAM1-765::natMX GFP-TUB1::LEU2 SPC110-Cherry::hphMX TRP1 pJT11	This study
EDY266-5B	a bik1-19 LYS2 SPC110-Cherry::hphMX TRP1 GFP-TUB1::URA3	This study
EDY265-2D	α bim1-16 DAM1 GFP-TUB1::LEU2 LYS2 SPC110-Cherry::hphMX	This study
EDY267-1B	α cik1-12 GFP-TUB1::LEU2 LYS2 NUF2 SPC110-Cherry::hphMX TRP1	This study
MMWY61	a CEN3::33LacO::KanMX pCUP1-GFP12LacI12::HIS3 LYS2 SPC110-Cherry::hphMX	Megan Wargacki
EDY252-4D	a CEN3::33LacO::KanMX DAM1-765::natMX pCUP1-GFP12LacI12::HIS3 LYS2 SPC110-Cherry::hphMX pJT11	This study
EDY252-10D	α CEN3::33LacO::KanMX cik1-12 pCUP1-GFP12LacI12::HIS3 LYS2 SPC110-Cherry::hphMX	This study
EDY252-19B	α CEN3::33LacO::KanMX cik1-12 DAM1-765::natMX pCUP1-GFP12LacI12::HIS3 LYS2 SPC110-Cherry::hphMX pJT11	This study

EDY257-3B	a bim1-16 CENIII::33LacO::KanMX pCUP1-GFP12LacI12::HIS3 LYS2 SPC110-Cherry::hphMX	This study
EDY258	α CEN3::33LacO::KanMX DAM1-765::natMX pCUP1-GFP12LacI12::HIS3 LYS2 SPC110-Cherry::hphMX	This study
EDY268-5B	a bim1-16 CEN3::33LacO::KanMX DAM1-765::natMX pCUP1-GFP12LacI12::HIS3 LYS2 SPC110-Cherry::hphMX pJT11	This study
EDY269-6A	α CEN3::33LacO::KanMX pCUP1-GFP12LacI12::HIS3 kar3-8 LYS2 or lys2Δ::HIS3 SPC110-Cherry::hphMX TRP1	This study
EDY269-6C	a CEN3::33LacO::KanMX DAM1-765::natMX pCUP1-GFP12LacI12::HIS3 kar3-8 LYS2 or lys2Δ::HIS3 SPC110-Cherry::hphMX TRP1	This study
EDY194-11B	a cik1-4A-GFP::KanMX LYS2 SPC110-Cherry::hphMX TRP1 CFP-TUB1::URA3	This study
EDY196-2D	α cik1-4A-GFP::KanMX DAM1-765::natMX LYS2 SPC110-Cherry::hphMX TRP1 CFP-TUB1::URA3	This study
EDY198-10D	a bim1-16 cik1-4A-GFP::KanMX leu2 LYS2 SPC110-Cherry::hphMX trp1 CFP-TUB1::URA3	This study
EDY226-1D	α cik1-4A HIS3 or his3-11,15 GFP-TUB1::LEU2 LYS2 SPC110-Cherry::hphMX TRP1	This study
EDY226-5D	a cik1-4A DAM1-765::natMX HIS3 or his3-11,15 GFP-TUB1::LEU2 LYS2 SPC110-Cherry::hphMX TRP1	This study
EDY213	a/α ADE3/ade3 LYS2/LYS2 pED26	This study
EDY214	a/α ADE3/ade3 LYS2/LYS2 pED30	This study

* all strains are in an *ade2-1 ade3*Δ *can1-100 his3-11,15 leu2-3,112 lys2*Δ*::HIS3 trp1-1 ura3-1* background unless otherwise noted.

Plasmid	Genotype	Source
pED2	2 μm ADE3 DAM1 LYS2	This study
pJT11	CEN6 DAM1 URA3	Jerry Tien
pED5	2 μm DAM1-765 URA3	This study
pSF15	2 μm DAM1 URA3	Susan Francis
pED26	CEN4 pCMD1-SKIP(1-13)-GFP URA3	This study
pED30	CEN4 pCMD1-SKIP(1-34)-GFP URA3	This study

Chapter IV

Future Directions and Summary

DAM1-765

I have shown that failure to attach kinetochores to microtubule plus ends results in potentially lethal misregulation of interpolar microtubules. This conclusion is based on the phenotype of partially-rescued *DAM1-765* double mutants. It would be useful to confirm this finding via analysis of the fully lethal phenotype itself. I have made an initial attempt at this analysis with temperature-sensitive *DAM1-765 kar3-8,* and the results are consistent with interpolar microtubule failure. Kar3 mutants carry the risk of displaying irrelevant phenotypes arising from disruption of Kar3/Vik1, however, so Cik1 would be a preferable target of study. A *cik1-12 DAM1-765* strain rescued by a degron-labeled *CIK1* allele could fill this role well.

It remains possible that one or more of the mutations derived in my screen prevents poleward walking of laterally-attached kinetochores. The notion of a kinetochore that is destined for a microtubule plus-end being walked in the opposite direction seems counterintuitive, so discovery of an allele that halts poleward walking would be an exciting find that would allow further study of this mysterious process in yeast. Similarly, one or more of the mutations may be deficient in maintaining lateral attachment regardless of poleward walking. The difference between lateral and end-on kinetochore-microtubule interactions is still poorly understood, but will be important to discover if we are ever to fully understand how the mitotic spindle captures and biorients kinetochores.

Both poleward-walking-deficient alleles and lateral-attachment-deficient alleles would be expected to have high rates of chromosome detachment in my partially-rescued double

mutants, so chromosomal detachment could be a good phenotype to look for to isolate the relevant strains. Fluorescently labeled Mad1, a spindle checkpoint component that in yeast localizes to kinetochores whose attachment has been abnormally delayed (Gillett et al., 2004), could serve as a marker of kinetochore attachment, allowing detection of attachment-deficient strains.

An alternative means of isolating lateral-attachment-deficient strains could be to examine GFP-labeled *CEN3* behavior. While studying *CEN3* biorientation in my various strains, I observed non-separated kinetochores being held tightly by one pole, then suddenly moving across the spindle to take up residence by the opposite pole. These instances likely represent kinetochore detachment and recapture events, and could be quantified. They could then be used as a readout of whether double mutant spindles are as efficient as single-mutants at maintaining their grip on kinetochores.

Cik1 and its SxIP Motif

I have shown in Chapter 3 that Cik1's SxIP motif is widely conserved and that mutation of it significantly affects Cik1 function. An obvious next step would be to directly demonstrate that Cik1 and Bim1 physically associate and that the SxIP motif is necessary for that association. This interaction could be demonstrated via quantitative Western blot and/or mass spectrometry of purified Bim1 and Cik1 in *CIK1* and *cik1-4A* backgrounds.

SxIP motifs are thought to function much more effectively in pairs (Honnappa et al., 2009). My experiments with fusing Cik1's SxIP motif to GFP could be optimized by providing GFP with a second SxIP motif, increasing the likelihood of demonstrating SxIP-based microtubule tip localization. Attaching a GST tag to my SxIP-GFP construct could provide that second SxIP motif by causing the resulting protein to dimerize.

I would also like to solve the mystery of whether Cik1's SxIP motif is involved in spindle elongation during all of anaphase B or just anaphase B phase 2. Crossing *cin8Δ* and *kip1Δ* alleles into a *cik1-4A-GFP* background could help determine the timing of Cik1 involvement. If *cik1-4A-GFP* spindles really never transition to anaphase B phase 2, I would expect *kip1Δ* to have little impact on its anaphase phenotype and *cin8Δ* to be more severe. If instead *cik1-4A-GFP* spindles do proceed through both phases of anaphase B, then each deletion should impact mainly the phase where its force production is dominant.

Summary

During mitosis, eukaryotic organisms universally attach kinetochores to microtubule plus ends. A structure as unstable as the plus end is a surprising site for such crucial attachments, especially considering that attachment there is not necessary for successful completion of mitosis (Shimogawa et al., 2006). I have shown that kinetochore residence at microtubule plus ends is important for ensuring proper development of interpolar microtubules. Spindles normally tolerate the loss of plus-end-bound kinetochores, but the additional loss of plus-end-binding proteins results in lethal misregulation of spindle microtubules.

Three proteins known to bundle interpolar microtubules in yeast, Bim1 and Kar3/Cik1 (Gardner et al., 2008), are only known to be capable of binding a single microtubule each. I have shown that Kar3/Cik1 contains a highly conserved N-terminal motif that assists in regulating anaphase spindle length and likely acts as a binding site for Bim1, potentially allowing the Kar3/Cik1 dimer to manipulate two microtubules at once (see Figure 4.1A). This ability to connect two microtubules could allow Kar3/Cik1 to not only bundle ipMTs together, but to participate in the balance of forces that regulate ipMT overlap and spindle length.

Kar3/Cik1 binding appears to be limited to microtubule plus ends (see Figure 4.1B). It therefore may exert an invariant inward force regardless of the degree of ipMT overlap, which suggests a simple self-regulating model for regulation of ipMT overlap. Bim1/Kar3/Cik1 could provide a constant inward-directed force promoting overlap increase. The plus-end-directed motors Cin8 and Kip1 bound to the microtubule lattice could provide a variable outward force. A too-large amount of overlap would provide a great deal of room for Cin8 and Kip1 binding, pushing the spindle poles outward, decreasing overlap, and therefore decreasing Cin8 and Kip1 force production. A too-small overlap would provide little room for Cin8 and Kip1 binding, allowing Bim1/Kar3/Cik1's inward force to dominate, increasing overlap and thereby increasing Cin8 and Kip1 force production. These kinesin motors may therefore maintain a stable degree of ipMT overlap, making overall spindle length dependent on microtubule length regulation.

Spindle construction during mitosis hinges on proper development of interpolar microtubules, which must be regulated differently during each stage of mitosis to allow the spindle to segregate chromosomes into each daughter cell. My work has contributed to our knowledge of interpolar microtubule regulation, thus increasing our understanding of a process that is fundamental to eukaryotic life.

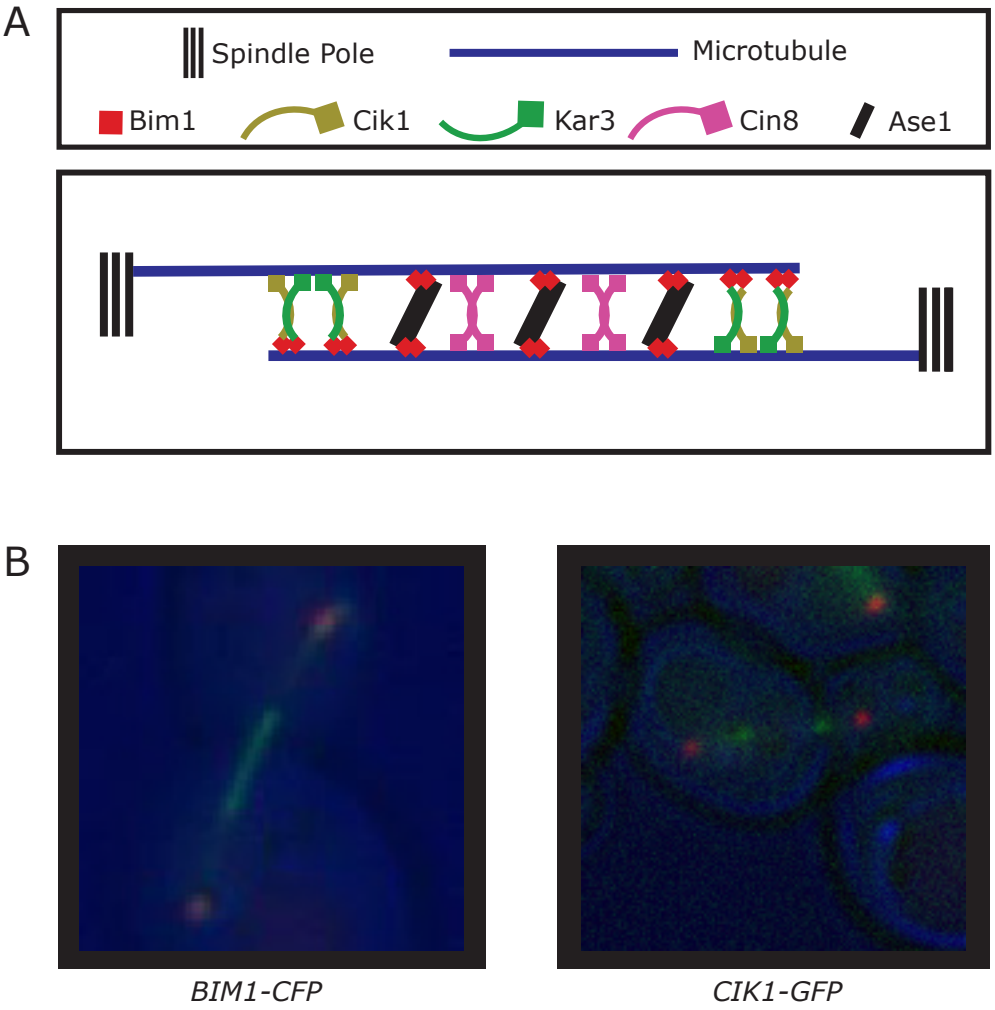

Figure 4.1: Model of Bim1, Cik1, and Kar3 interpolar microtubule bundling. A: Diagram of ipMT bundling. Kip1 is largely redundant with Cin8 and is not shown. Motor domains of Cik1, Cin8, and Kar3 are represented as squares. Plus-end-directed walking of Cin8 produces spindle-elongating forces that are balanced by minus-end-directed walking of Bim1/Kar3/Cik1 at ipMT plus ends. B: Images of *BIM1-CFP* and *CIK1-GFP* distribution during anaphase. Spindle poles are labeled in red. Bim1 is concentrated in the mid-spindle in an area that may represent the region of ipMT overlap. Kar3/Cik1 instead localizes to 2-4 foci that may represent ipMT plus ends.

Bibliography

Akhmanova, A., and Steinmetz, M.O. (2008). Tracking the ends: a dynamic protein network controls the fate of microtubule tips. Nature Reviews: Molecular Cell Biology *9*, 309-322.

Allingham, J.S., Sproul, L.R., Rayment, I., and Gilbert, S.P. (2007). Vik1 modulates microtubule-Kar3 interactions through a motor domain that lacks an active site. Cell *128*, 1161-1172.

Asbury, C.L., Gestaut, D.R., Powers, A.F., Franck, A.D., and Davis, T.N. (2006). The Dam1 kinetochore complex harnesses microtubule dynamics to produce force and movement. Proc Natl Acad Sci U S A *103*, 9873-9878.

Barrett, J.G., Manning, B.D., and Snyder, M. (2000). The Kar3p kinesin-related protein forms a novel heterodimeric structure with its associated protein Cik1p. Molecular Biology of the Cell *11*, 2373-2385.

Benanti, J.A., Matyskiela, M.E., Morgan, D.O., and Toczyski, D.P. (2009). Functionally distinct isoforms of Cik1 are differentially regulated by APC/C-mediated proteolysis. Molecular Cell *33*, 581-590.

Berlin, V., Styles, C.A., and Fink, G.R. (1990). BIK1, a protein required for microtubule function during mating and mitosis in Saccharomyces cerevisiae, colocalizes with tubulin. J Cell Biol *111*, 2573-2586.

Blake-Hodek, K.A., Cassimeris, L., and Huffaker, T.C. (2010). Regulation of microtubule dynamics by Bim1 and Bik1, the budding yeast members of the EB1 and CLIP-170 families of plus-end tracking proteins. Molecular Biology of the Cell *21*, 2013-2023.

Braun, M., Lanksy, Z., Fink, G., Ruhnow, F., Diez, S., and Janson, M.E. (2011). Adaptive braking by Ase1 prevents overlapping microtubules from sliding completely apart. Nature Cell Biology *13*, 1259-1264.

Chan, G.K., Liu, S.-T., and Yen, T.J. (2005). Kinetochore structure and function. Trends in Cell Biology *15*, 589-598.

Cheeseman, I.M., Anderson, S., Jwa, M., Green, E.M., Kang, J., Yates, J.R., 3rd, Chan, C.S., Drubin, D.G., and Barnes, G. (2002). Phospho-regulation of kinetochore-microtubule attachments by the Aurora kinase Ipl1p. Cell *111*, 163-172.

Cimini, D., Wan, X., Hirel, C.B., and Salmon, E.D. (2006). Aurora kinase promotes turnover of kinetochore microtubules to reduce chromosome segregation errors. Current Biology *16*, 1711-1718.

Dujardin, D., Wacker, U.I., Moreau, A., Schroer, T.A., Rickard, J.E., and De Mey, J.R. (1998). Evidence for a role of CLIP-170 in the establishment of metaphase chromosome alignment. Journal of Cell Biology *141*, 849-862.

Gachet, Y., Reyes, C., Courthéoux, T., Goldstone, S., Gay, G., Serrurier, C., and Tournier, S. (2008). Sister kinetochore recapture in fission yeast occurs by two distinct mechanisms, both requiring Dam1 and Klp2. Molecular Biology of the Cell *19*, 1646-1662.

Gardner, M.K., Haase, J., Mythreye, K., Molk, J.N., Anderson, M., Joglekar, A.P., O'Toole, E.T., Winey, M., Salmon, E.D., Odde, D.J.*, et al.* (2008). The microtubule-based motor Kar3 and plus end-binding protein Bim1 provide structural support for the anaphase spindle. The Journal of Cell Biology *180*, 91-100.

Geiser, J.R., van-Tuinen, D., Brockerhoff, S.E., Neff, M.M., and Davis, T.N. (1991). Can calmodulin function without binding calcium? Cell *65*, 949-959.

Gestaut, D.R., Graczyk, B., Cooper, J., Widlund, P.O., Zelter, A., Wordeman, L., Asbury, C.L., and Davis, T.N. (2008). Phosphoregulation and depolymerization-driven movement of the Dam1 complex do not require ring formation. Nat Cell Biol *10*, 407-414.

Gillett, E.S., Espelin, C.W., and Sorger, P.K. (2004). Spindle checkpoint proteins and chromosome-microtubule attachment in budding yeast. J Cell Biol *164*, 535-546.

Goshima, G., Nédélec, F., and Vale, R.D. (2005). Mechanisms for focusing mitotic spindle poles by minus end-directed motor proteins. Journal of Cell Biology *171*, 229-240.

Goshima, G., and Scholey, J.M. (2010). Control of mitotic spindle length. Annual Review of Cell and Developmental Biology *26*, 21-57.

Gulick, A.M., Song, H., Endow, S.A., and Rayment, I. (1998). X-Ray crystal structure of the yeast Kar3 motor domain complexed with Mg·ADP to 2.3 Å resolution. Biochemistry *37*, 1769-1776.

Hagan, I., and Yanagida, M. (1990). Novel potential mitotic motor protein encoded by the fission yeast cut7+ gene. Nature *347*, 563-566.

Honnappa, S., Gouveia, S.M., Weisbrich, A., Damberger, F.F., Bhavesh, N.S., Jawhari, H., Grigoriev, I., van Rijssel, F.J., Buey, R.M., Lawera, A.*, et al.* (2009). An EB1-binding motif acts as a microtubule tip localization signal. Cell *138*, 366-376.

Honnappa, S., John, C.M., Kostrewa, D., Winkler, F.K., and Steinmetz, M.O. (2005). Structural insights into the EB1-APC interaction. The EMBO Journal *24*, 261-269.

Hoyt, M.A., He, L., Loo, K.K., and Saunders, W.S. (1992). Two *Saccharomyces cerevisiae* kinesin-related gene products required for mitotic spindle assembly. J Cell Biol *118*, 109-120.

Janson, M.E., Loughlin, R., Loïodice, I., Fu, C., Brunner, D., Nédélec, F.J., and Tran, P.T. (2007). Crosslinkers and motors organize dynamic microtubules to form stable bipolar arrays in fission yeast. Cell *128*, 357-368.

Jin, F., Liu, H., Li, P., Yu, H.-G., and Wang, Y. (2012). Loss of function of the Cik1/Kar3 motor complex results in chromosomes with syntelic attachment that are sensed by the tension checkpoint. PLoS Genetics *8*, e1002492.

Kotwaliwale, C.V., Buvelot Frei, S., Stern, B.M., and Biggins, S. (2007). A pathway containing the Ipl1/Aurora protein kinase and the spindle midzone protein Ase1 regulates yeast spindle assembly. Developmental Cell *13*, 433-445.

Lampson, M.A., and Cheeseman, I.M. (2011). Sensing centromere tension: Aurora B and the regulation of kinetochore function. Trends in Cell Biology *21*, 133-140.

Lampson, M.A., Renduchitala, K., Khodjakov, A., and Kapoor, T.M. (2004). Correcting improper chromosome-spindle attachments during cell division. Nature Cell Biology *6*, 232-237.

Lawrence, C.J., Dawe, R.K., Christie, K.R., Cleveland, D.W., Dawson, S.C., Endow, S.A., Goldstein, L.S.B., Goodson, H.V., Hirokawa, N., Howard, J.*, et al.* (2004). A standardized kinesin nomenclature. Journal of Cell Biology *167*, 19-22.

Li, Y., Bachant, J., Alcasabas, A.A., Wang, Y., Qin, J., and Elledge, S.J. (2002). The mitotic spindle is required for loading of the DASH complex onto the kinetochore. Genes Dev *16*, 183-197.

Mackey, A.T., and Gilbert, S.P. (2003). The ATPase cross-bridge cycle of the Kar3 motor domain. Implications for single head motility. J Biol Chem *278*, 3527-3535.

Maddox, P.S., Bloom, K.S., and Salmon, E.D. (2000). The polarity and dynamics of microtubule assembly in the budding yeast Saccharomyces cerevisiae. Nat Cell Biol *2*, 36-41.

Mana-Capelli, S., McLean, J.R., Chen, C.T., Gould, K.L., and McCollum, D. (2012). The kinesin-14 Klp2 is negatively regulated by the SIN for proper spindle elongation and telophase nuclear positioning. Molecular biology of the cell *23*, 4592-4600.

Manning, B.D., Barrett, J.G., Wallace, J.A., Granok, H., and Snyder, M. (1999). Differential regulation of the Kar3p kinesin-related protein by two associated proteins, Cik1p and Vik1p. J Cell Biol *144*, 1219-1233.

Manning, B.D., and Snyder, M. (2000). Drivers and passengers wanted! The role of kinesin-associated proteins. Trends in Cell Biology *10*, 281-289.

McIntosh, J., Roos, U., Neighbors, B., and McDonald, K. (1985). Architecture of the microtubule component of mitotic spindles from *Dictyostelium discoideum*. Journal of Cell Science *75*, 93-129.

Meluh, P.B., and Rose, M.D. (1990). KAR3, a kinesin-related gene required for yeast nuclear fusion [published erratum appears in Cell 1990 May 4;61(3):548]. Cell *60*, 1029-1041.

Miranda, J.J., De Wulf, P., Sorger, P.K., and Harrison, S.C. (2005). The yeast DASH complex forms closed rings on microtubules. Nat Struct Mol Biol *12*, 138-143.

Muller, E.G. (1996). A glutathione reductase mutant of yeast accumulates high levels of oxidized glutathione and requires thioredoxin for growth. Mol Biol Cell *7*, 1805-1813.

Nicklas, R.B., and Ward, S.C. (1994). Elements of error correction in mitosis: microtubule capture, release, and tension. J Cell Biol *126*, 1241-1253.

Nigavekar, S.S., and Cannon, J.F. (2002). Characterization of genes that are synthetically lethal with *ade3* or *leu2* in *Saccharomyces cerevisiae*. Yeast *19*, 115-122.

Ortiz, J., Funk, C., Schäfer, A., and Lechner, J. (2009). Stu1 inversely regulates kinetochore capture and spindle stability. Genes and Development *23*, 2778-2791.

Page, B.D., and Snyder, M. (1992). CIK1: a developmentally regulated spindle pole body-associated protein important for microtubule functions in Saccharomyces cerevisiae. Genes Dev *6*, 1414-1429.

Pinsky, B.A., and Biggins, S. (2005). The spindle checkpoint: tension versus attachment. Trends Cell Biol *15*, 486-493.

Pinsky, B.A., Kung, C., Shokat, K.M., and Biggins, S. (2006). The Ipl1-Aurora protein kinase activates the spindle checkpoint by creating unattached kinetochores. Nat Cell Biol *8*, 78-83.

Powers, A.F., Franck, A.D., Gestaut, D.R., Cooper, J., Gracyzk, B., Wei, R.R., Wordeman, L., Davis, T.N., and Asbury, C.L. (2009). The Ndc80 kinetochore complex forms load-bearing attachments to dynamic microtubule tips via biased diffusion. Cell *136*, 865-875.

Rieder, C.L., and Alexander, S.P. (1990). Kinetochores are transported poleward along a single astral microtubule during chromosome attachment to the spindle in newt lung cells. J Cell Biol *110*, 81-95.

Rothstein, R. (1991). Targeting, disruption, replacement, and allele rescue: Integrative DNA transformation in yeast. Meth Enzymol *194*, 281-301.

Salmon, E.D. (2005). Microtubules: a ring for the depolymerization motor. Curr Biol *15*, R299-302.

Saunders, W., Lengyel, V., and Hoyt, M.A. (1997). Mitotic spindle function in Saccharomyces cerevisiae requires a balance between different types of kinesin-related motors. Mol Biol Cell *8*, 1025-1033.

Saunders, W.S., and Hoyt, M.A. (1992). Kinesin-related proteins required for structural integrity of the mitotic spindle. Cell *70*, 451-458.

Sherman, F., Fink, G.R., and Hicks, J.B. (1986). Methods in Yeast Genetics (Cold Spring Harbor, New York: Cold Spring Harbor Laboratory).

Shimogawa, M.M., Graczyk, B., Gardner, M.K., Francis, S.E., White, E.A., Ess, M., Molk, J.N., Ruse, C., Niessen, S., Yates, J.R., 3rd*, et al.* (2006). Mps1 phosphorylation of Dam1 couples kinetochores to microtubule plus ends at metaphase. Curr Biol *16*, 1489-1501.

Shimogawa, M.M., Wargacki, M.M., Muller, E.G., and Davis, T.N. (2010). Laterally attached kinetochores recruit the checkpoint protein Bub1, but satisfy the spindle checkpoint. Cell Cycle *9*, 3619-3628.

Slep, K., and Vale, R. (2007). Structural basis of microtubule plus end tracking by XMAP215, CLIP-170, and EB1. Molecular Cell *27*, 976-991.

Sproul, L.R., Anderson, D.J., Mackey, A.T., Saunders, W.S., and Gilbert, S.P. (2005). Cik1 targets the minus-end kinesin depolymerase kar3 to microtubule plus ends. Curr Biol *15*, 1420-1427.

Storici, F., and Resnick, M.A. (2006). The *Delitto Perfetto* approach to *in vivo* site-directed mutagenesis and chromosome rearrangements with synthetic oligonucleotides in yeast. Methods in Enzymology *409*, 329-345.

Straight, A.F., Sedat, J.W., and Murray, A.W. (1998). Time-lapse microscopy reveals unique roles for kinesins during anaphase in budding yeast. J Cell Biol *143*, 687-694.

Sullivan, D.S., and Huffaker, T.C. (1992). Astral microtubules are not required for anaphase B in *Saccharomyces cerevisiae*. J Cell Biol *119*, 379-388.

Tanaka, K., Kitamura, E., Kitamura, Y., and Tanaka, T.U. (2007). Molecular mechanisms of microtubule-dependent kinetochore transport toward spindle poles. J Cell Biol *178*, 269-281.

Tanaka, K., Mukae, N., Dewar, H., van Breugel, M., James, E.K., Prescott, A.R., Antony, C., and Tanaka, T.U. (2005). Molecular mechanisms of kinetochore capture by spindle microtubules. Nature *434*, 987-994.

Tanaka, T.U., and Desai, A. (2008). Kinetochore-microtubule interactions: the means to the end. Current Opinion in Cell Biology *20*, 53-63.

Tanenbaum, M.E., Galjart, N., van Vugt, M.A., and Medema, R.H. (2006). CLIP-170 facilitates the formation of kinetochore-microtubule attachments. The EMBO Journal *25*, 45-57.

Tien, J.F., Umbreit, N.T., Gestaut, D.R., Franck, A.D., Cooper, J., Wordeman, L., Gonen, T., Asbury, C.L., and Davis, T.N. (2010). Cooperation of the Dam1 and Ndc80 kinetochore complexes enhances microtubule coupling and is regulated by aurora B. J Cell Biol *189*, 713-723.

Venkitaraman, A.R. (2007). Chromosomal instability in cancer: causality and interdependence. Cell Cycle *6*, 2341-2343.

Weisbrich, A., Honnappa, S., Jaussi, R., Okhrimenko, O., Frey, D., Jelesarov, I., Akhmanova, A., and Steinmetz, M.O. (2007). Structure-function relationship of CAP-Gly domains. Nature Structural & Molecular Biology *14*, 959-967.

Westermann, S., Avila-Sakar, A., Wang, H.W., Niederstrasser, H., Wong, J., Drubin, D.G., Nogales, E., and Barnes, G. (2005). Formation of a dynamic kinetochore- microtubule interface through assembly of the Dam1 ring complex. Mol Cell *17*, 277-290.

Wilson, E.B. (1925). The Cell in Development and Heredity, 3rd edn (New York: Macmillan).

Winey, M., Mamay, C.L., O'Toole, E.T., Mastronarde, D.N., Giddings Jr., T.H., McDonald, K.L., and McIntosh, J.R. (1995). Three-dimensional ultrastructural analysis of the *Saccharomyces cerevisiae* mitotic spindle. J Cell Biol *129*, 1601-1615.

Wolyniak, M.J., Blake-Hodek, K., Kosco, K., Hwang, E., You, L., and Huffaker, T.C. (2006). The regulation of microtubule dynamics in Saccharomyces cerevisiae by three interacting plus-end tracking proteins. Mol Biol Cell *17*, 2789-2798.

Yin, H., You, L., Pasqualone, D., Kopski, K.M., and Huffaker, T.C. (2002). Stu1p is physically associated with β-Tubulin and is required for structural integrity of the mitotic spindle. Molecular Biology of the Cell *13*, 1881-1892.

Zaichick, S.V., Metodiev, M.V., Nelson, S.A., Durbrovskyi, O., Draper, E., Cooper, J.A., and Stone, D.E. (2009). The mating-specific Gα interacts with a kinesin-14 and regulates phermone-induced nuclear migration in budding yeast. Molecular Biology of the Cell *20*, 2820-2830.

Eliott Robison Davidson

Curriculum Vitae

EDUCATION

Doctor of Philosophy – Molecular and Cellular Biology (2013)
University of Washington, Seattle WA
Dissertation: Regulation of interpolar microtubules by plus-end binding proteins in *Saccharomyces cerevisiae*
Advisor: Dr. Trisha Davis

Bachelor of Arts – Biology (2005)
University of Utah, Salt Lake City UT

PUBLICATIONS

White, JQ, Nicholas, TJ, Gritton, J, Truong, L, **Davidson, ER**, and Jorgensen, EM. (2007) *The sensory circuitry for sexual attraction in C. elegans males.* Current Biology 17(21):1847-1857.

MEETINGS

American Society for Cell Biology Annual Meeting (2012)
Poster Presentation: *A SxIP motif in the budding yeast kinesin Kar3/Cik1 is necessary for anaphase spindle elongation*

American Society of Cell Biology Annual Meeting (2011)
Poster Presentation: *The budding yeast kinesin Kar3/Cik1 corrals interpolar microtubule plus ends during mitosis*

Genetics Society of America Yeast Genetics and Molecular Biology Meeting (2010)
Poster Presentation: *A synthetic lethal screen against a mutant defective for end-on kinetochore-microtubule binding*

TEACHING

Teaching Assistant – Biology 200 (Winter 2008)
Department of Biology, University of Washington, Seattle WA

Teaching Assistant – Genome 371 (Summer 2007)
Department of Genome Sciences, University of Washington, Seattle WA